Mathematics

https://www.aimspress.com/journal/Math

AIMS Mathematics, 11(9): 27969–28008.
DOI:10.3934/math.20261117
Received: 10 April 2026
Revised: 21 August 2026
Accepted: 25 August 2026
Published: 02 September 2026

Research article

Observer-based boundary stabilization of a reaction–diffusion equation under random measurement deception: a dynamic event-triggered design

Lianglin Xiong[1,2], Xueqing Chen[1,*], Haiyang Zhang[1] and Tao Wu[3]

[1] School of Mathematics and Computer Science, Yunnan Minzu University, Kunming 650504, Yunnan, China

[2] Yunnan Open University, Kunming 650504, Yunnan, China

[3] School of Mathematics and Statistics, Yunnan University, Kunming 650504, Yunnan, China

* **Correspondence:** Email: 24213037570006@ymu.edu.cn.

Abstract: This work considers dynamic event-triggered boundary output feedback control for a one-dimensional reaction–diffusion equation when the boundary measurement may be randomly falsified. The compromised measurement channel is described by a Bernoulli switching model together with a Lipschitz nonlinear deception mapping. To alleviate the control update and actuation burden in networked implementation, a dynamic triggering law equipped with an auxiliary internal state is introduced so that the triggering threshold is adjusted online according to the closed-loop evolution. It is further shown that the triggering instants admit a uniform positive separation, thereby excluding Zeno accumulation. Based on this triggering framework, a backstepping boundary observer and its corresponding boundary feedback law are constructed. A composite Lyapunov analysis is then carried out to establish sufficient conditions for a global mean-square exponential estimate of the plant and observer states with respect to the augmented initial energy despite the coexistence of random deception and event-triggered updating. Numerical simulations, including Monte Carlo tests under independent attack realizations, are finally provided to illustrate the theoretical results. The results show that the proposed scheme stabilizes the originally unstable reaction–diffusion system, maintains effective state estimation under intermittent deceptive measurements, guarantees a positive interevent time, and substantially reduces unnecessary boundary control updates while preserving the desired closed-loop convergence behavior.

Keywords: reaction–diffusion equation; boundary observer; event-triggered boundary control; deceptive measurement attacks; global mean-square exponential stability
Mathematics Subject Classification: 35K57, 93C20, 93D15

1. Introduction

Boundary observation for partial differential equation (PDE) systems aims to reconstruct the spatially distributed state using only measurements available at the boundary, which is a typical sensing paradigm due to practical accessibility constraints [1, 2]. Boundary control stabilizes and regulates infinite-dimensional dynamics by injecting control inputs through boundary conditions, which is often more consistent with practical actuation than in-domain actuation for many engineering systems [3, 4]. This boundary-sensing and actuation paradigm offers advantages such as low cost, ease of implementation, and high engineering feasibility, but it also entails intrinsic difficulties. Boundary operators are typically unbounded, and closed-loop behavior is significantly influenced by spatial energy propagation, so stability and performance analysis must be carried out within an operator framework and based on energy estimates rather than by a straightforward extension of matrix-based tools for finite-dimensional systems [4, 5]. The need for boundary observation and boundary control arises broadly in application scenarios including heat conduction and reaction–diffusion processes, transport and flow systems in channels or pipelines, and vibration suppression of flexible structures, where sensors and actuators are naturally placed only at accessible boundaries [2,6]. More broadly, reaction–diffusion equations provide a versatile framework for describing complex spatiotemporal phenomena, including spatial heterogeneity, taxis and nonlocal interactions, and delay-induced pattern formation in distributed biological systems [7, 8]. Among various constructive design methods, the backstepping approach is regarded as a systematic tool: Through Volterra integral transformations characterized by kernel functions, the original system, or equivalently the observer error subsystem, can be recast into a reference system possessing desired stability features, from which boundary feedback laws and boundary observers under Neumann or Robin boundary conditions can be systematically derived [4, 9, 10]. Building on this foundation, a natural and practically meaningful next step is to further incorporate the sampling and communication constraints imposed by networked boundary sensing and boundary actuation, which motivates the subsequent discussion on event-triggering mechanisms [11–13].

Event-triggered control refers to a feedback updating mechanism that updates the control input or transmits measurement information according to whether a prescribed event condition is satisfied; sampling and updating are performed only when the system state or output meets a predesigned triggering rule (or the triggering function reaches a given threshold) [11, 14]. Its prominent advantage is that it can significantly reduce unnecessary periodic sampling and communication while maintaining closed-loop performance and stability, and it is therefore well suited for resource-constrained networked control scenarios such as limited bandwidth, energy-sensitive devices, or shared communication links [11, 12, 15]. In recent years, event triggering has developed into a relatively systematic research framework for finite-dimensional systems, with substantial progress on triggering rule construction, output feedback and dynamic trigger design, robustness analysis, and minimum dwell time characterizations for avoiding Zeno behavior [15–17]. However, extending event-triggered ideas to PDE systems is typically more challenging [18–20]. On one hand, PDE dynamics are infinite dimensional, and triggering conditions often involve energy-type functionals of spatially distributed states and boundary terms, which makes it difficult to directly reuse matrix inequality tools or pointwise error bounds developed for finite-dimensional models [18, 19]. On the other hand, boundary sensing and boundary actuation correspond to unbounded operators, and when sample-and-hold effects and network-induced errors are taken into account, closed-loop stability proofs and Zeno-free design become technically more challenging [13, 20, 21]. In this context, it is natural and practically meaningful to further consider abnormal and malicious disturbances on networked boundary measurement channels such as deceptive data injection attacks [22–24]. In this paper, the attack process is represented by a Bernoulli-type random variable, and the corrupted measurement is characterized through a deception map satisfying a Lipschitz condition [25, 26].

In networked boundary observation and boundary actuation, boundary measurements are transmitted over communication links to the controller or the observer, rendering the sensing channel vulnerable to exogenous disturbances and malicious interference [22, 27]. Deception attacks aim to mislead estimation and control by forging, replacing, or nonlinearly manipulating measurement data without necessarily acting directly on the plant [23, 27]. Such falsified boundary measurements may significantly degrade closed-loop stability and performance, particularly for distributed parameter systems where only a few boundary sensors are available, and the boundary measurement is often the sole correction source for feedback and observer correction [6, 28]. To capture the random nature of attack occurrence while retaining an analyzable corruption model, we introduce a Bernoulli random variable to indicate whether an attack occurs and model the received boundary measurement as a random switching between the genuine output and a falsified signal generated by a Lipschitz deception map [25, 26]. This formulation accommodates a class of amplitude-scaling and state-dependent nonlinear distortions satisfying the prescribed relative bound and facilitates a unified mean-square, energy estimate-based analysis of observer error propagation, thereby laying the foundation for the subsequent design of attack-resilient, observer-based, event-triggered boundary control mechanisms [28, 29].

Most existing studies on event-triggered PDE control concentrate on resource-aware scheduling and sampled-data implementations in attack-free settings, typically under the assumption of reliable measurements or the availability of full-state or complete output information [29–31]; as a result, triggering analyses are typically centered on stability and Zeno-free guarantees [32, 33]. Meanwhile, observer and backstepping designs for PDE systems have developed into a relatively mature constructive framework [9, 10]; however, most results still rely on continuous-time measurements and continuously updated output injection mechanisms, with comparatively limited attention to the sample-and-hold control updates and implementation errors introduced by networked sampling [13, 29]. By comparison, the literature on deception attacks and secure control is still concentrated mainly on finite-dimensional models [25–27], although a number of recent studies have started to consider distributed parameter and PDE settings [28]. However, they typically emphasize attack detection, robust estimation, or continuous-time resilient control, and they rarely integrate random deception attacks with event-triggered boundary-actuation mechanisms and boundary observer-based, closed-loop designs in a unified manner [34]. As a consequence, a mathematically unified framework that simultaneously incorporates boundary observation, event-triggered control updating, and random deceptive measurement attacks while establishing both Zeno-free triggering behavior and mean-square closed-loop stability is still lacking.

Motivated by the above observations, we consider a reaction–diffusion system with randomly corrupted boundary measurements and develop an observer-based, dynamic event-triggered strategy for its boundary stabilization. In contrast to the existing attack-free studies on event-triggered boundary control for parabolic PDEs, the setting considered here simultaneously involves boundary observation, sampled data or event-triggered implementation, and random deception acting on the measurement channel. A central analytical challenge arises because the falsified measurement enters the observer correction through random switching, whereas the triggering law introduces both an additional internal dynamic variable and a sample-and-hold error into the closed-loop dynamics. Consequently, the estimation error subsystem, the triggering mechanism, and the PDE energy analysis become intrinsically coupled. To overcome this difficulty, we combine Volterra backstepping transformations, a dynamic event-triggering mechanism, and a composite Lyapunov analysis within a unified framework so that the attack-induced measurement deviation, sample-and-hold error, observer error, and internal triggering dynamics can be treated jointly in the subsequent stability and Zeno-free analyses. The main contributions are summarized below.

- For a one-dimensional reaction–diffusion system with random deceptive measurement attacks, we design an observer-based, event-triggered boundary control framework. The attack process is characterized by a Bernoulli switching law together with a Lipschitz deception map so that corrupted boundary observations can be incorporated explicitly into both the observer-controller structure and the subsequent stability analysis.
- For the attacked boundary control setting, we design a fully dynamic triggering rule by introducing an auxiliary internal variable coupled with the sample-and-hold implementation error. Under this mechanism, a uniform positive lower bound on the interevent times is established, thereby excluding Zeno behavior and providing a mathematically justified update rule for networked boundary actuation under uncertain measurements.
- By integrating backstepping transformations, PDE energy arguments, and pathwise estimates, we develop a composite Lyapunov framework that captures the interaction among the system state, the estimation error, and the internal triggering dynamics. On this basis, verifiable sufficient conditions are obtained to ensure a global mean-square exponential estimate for the plant and observer states with respect to the augmented initial energy in the simultaneous presence of random deception attacks and event-triggered updates.

The remainder of this paper is arranged as follows. Section 2 describes the system model, the deception attack modeling on the boundary measurement channel, and the associated assumptions and preliminaries. Section 3 develops the backstepping-based boundary observer and boundary control law, derives the equivalent error system, and analyzes key properties of the kernel functions. Section 4 proposes a dynamic event-triggering strategy, derives a minimum dwell time lower bound, and proves the Zeno-free behavior. Section 5 constructs a composite Lyapunov functional and establishes sufficient conditions for a global mean-square exponential estimate of the plant and observer states with respect to the augmented initial energy. Section 6 provides numerical simulations to illustrate the closed-loop performance and triggering behavior of the proposed method under deceptive measurements. Finally, Section 7 summarizes this article and explains the future research directions.

Notation: $\mathbb{R}$ and $\mathbb{R}_+$ denote the sets of real and non-negative real numbers, respectively. $L^2(0,1)$ denotes the Hilbert space of square-integrable functions on $(0,1)$ with norm $\|f\| := \left(\int_0^1 f^2(x)dx\right)^{1/2}$. $H^1(0,1)$ denotes the Sobolev space of functions in $L^2(0,1)$ whose weak derivative belongs to $L^2(0,1)$. For a function $f(x,t)$, we use the shorthand notation $f[t] := f(\cdot,t)$ and $\|f[t]\| := \|f(\cdot,t)\|_{L^2(0,1)}$. The notation $|\cdot|_\infty$ denotes the essential supremum norm. $|\mathbf{a}|$ denotes the Euclidean norm if a is a vector and the absolute value if a is scalar. $\mathbb{E}$ denotes mathematical expectation. The symbol C_i represents a positive constant whose value may vary from one occurrence to another. The Volterra kernels $P(x, y)$ and $K(x, y)$ are defined on the triangular domain $(x, y) \in [0, 1]^2 : 0 \leq y \leq x \leq 1$. The Bernoulli random variable $\beta(t_k) \in \{0, 1\}$ specifies the deception mode associated with the interevent interval starting at the control update instant t_k.

2. Problem statement and preliminaries

2.1. System description

We focus on the reaction–diffusion system

$$v_t(x, t) = \varepsilon v_{xx}(x, t) + \lambda v(x, t), \quad (x, t) \in (0, 1) \times \mathbb{R}_+, \tag{2.1}$$

subject to boundary conditions

$$v_x(0, t) = 0, \quad t \geq 0, \tag{2.2}$$

$$v_x(1, t) + qv(1, t) = U(t), \quad t \geq 0, \tag{2.3}$$

and

$$v(x, 0) = v_0(x), \quad x \in (0, 1), \tag{2.4}$$

where $v(x, t)$ denotes the state; $\varepsilon > 0$ and $\lambda > 0$ represent the diffusion and reaction coefficients, respectively; $q > 0$ is the Robin boundary parameter; and $U(t)$ denotes the boundary actuation imposed at $x = 1$. We write $\mathbb{R}_+ := [0, \infty)$.

The considered model is a one-dimensional linear parabolic distributed-parameter system, characterized by the coexistence of second-order spatial diffusion and linear reaction dynamics, with the control input applied through the Robin boundary condition at $x = 1$. We study System (2.1)–(2.4) in the Hilbert space $L^2(0, 1)$. Let $A\phi := \varepsilon\phi'' + \lambda\phi$ with the homogeneous boundary conditions $\phi'(0) = 0$ and $\phi'(1) + q\phi(1) = 0$. It is well-known that the diffusion operator under Neumann–Robin boundary conditions gives rise to an analytic C_0-semigroup on $L^2(0, 1)$; moreover, the nonhomogeneous Robin boundary input in (2.3) can be handled via a standard lifting transformation. Consequently, for any $v_0 \in L^2(0, 1)$ and any admissible (e.g., piecewise continuous) boundary input $U(t)$, System (2.1)–(2.4) has a unique mild solution in $L^2(0, 1)$ for all $t \geq 0$; under the usual additional regularity assumptions, boundary traces are well-defined, which justifies the subsequent backstepping and Lyapunov analysis.

One introduces a standard stabilizability condition as follows:

Assumption 1. *[29] The parameters satisfy*

$$q > \frac{\lambda + \varepsilon}{2\varepsilon}. \tag{2.5}$$

According to the condition in Assumption 1, the kernel boundary value problem arising in the backstepping design admits a unique Volterra solution, and the resulting boundary feedback is able to exponentially stabilize the open-loop plant. Then, by defining

$$r = q - \frac{\lambda}{2\varepsilon}, \tag{2.6}$$

Assumption 1 means $r > 1/2$, which will be repeatedly applied to obtain coercive energy estimations.

Remark 1. *Throughout the paper, we work under standard regularity conditions (* $v_0, \hat{v}_0 \in H^1(0,1)$ *and piecewise* C^1 *signals involved in the boundary actuation or estimation) so that the boundary traces* $v(0,t)$*,* $\hat{v}(0,t)$ *are well-defined, and the integrations by parts used in the subsequent derivations are valid.*

The boundary measurement available to the observer is

$$y_b(t) = v(0,t), \quad t \geq 0, \tag{2.7}$$

which is sent over a possibly insecure communication link.

2.2. Deceptive attacks on the measurement signal

We assume that the boundary measurement $y_b(t)$ may be altered by an adversary before it is used by the observer. In modern networked control of distributed parameter systems, the sensing data are often transmitted over open or partially protected channels and may therefore be vulnerable to intentional falsification. Let $y_r(t)$ denote the signal actually received by the observer. One can express the received measurement as

$$y_r(t) = \beta(t)y_b(t) + (1-\beta(t))\varphi(y_b(t)), \tag{2.8}$$

where $\varphi(\cdot)$ is a nonlinear deception map, and $\beta(t) \in \{0,1\}$ is a Bernoulli random variable indicating whether the transmitted measurement is genuine or falsified. Specifically, when $\beta(t) = 1$, no attack occurs, and $y_r(t) = y_b(t)$, whereas when $\beta(t) = 0$, the received signal is forged according to $y_r(t) = \varphi(y_b(t))$.

Let $\{t_k\}_{k\in\mathbb{N}}$ denote the control update instants generated by the dynamic event-triggering mechanism introduced later in Section 4. To model interval-consistent random deception, we assume that at each control update instant t_k, a fresh Bernoulli variable $\beta(t_k)$ is sampled independently of the closed-loop history prior to t_k with

$$\mathbb{E}\{\beta(t_k)\} = P_g \in (0,1). \tag{2.9}$$

Here, $\mathbb{E}\{\cdot\}$ represents the mathematical expectation taken with respect to the probability space associated with the attack process. The parameter P_g represents the probability that the genuine measurement mode is active on the interevent interval starting at t_k, corresponding to $\beta(t_k) = 1$, whereas $1 - P_g$ represents the probability that the received measurement is deceptively falsified, corresponding to $\beta(t_k) = 0$. Therefore, a larger value of P_g indicates a more reliable measurement channel, whereas a smaller value of P_g corresponds to a higher probability of deceptive measurements.

We further impose the following interval consistency assumption on the attack process.

Assumption 2 (Interval-consistent attacks)**.** *Let* $\{t_k\}_{k\in\mathbb{N}}$ *represent the event times, where* $t_0 = 0$*, and* $t_{k+1} > t_k$*. The Bernoulli attack indicator* $\beta(t) \in \{0,1\}$ *is assumed to be* piecewise constant *on each interevent interval; that is,*

$$\beta(t) = \beta(t_k), \qquad t \in [t_k, t_{k+1}),\ k \in \mathbb{N}. \tag{2.10}$$

This assumption reflects the fact that an attacker typically maintains a fixed falsification pattern over each interevent interval rather than switching arbitrarily fast within an interevent interval.

Remark 2. *The interval consistency requirement in* (2.10) *is imposed to obtain a tractable attack model over the event-triggered control update intervals. It does not preclude more aggressive adversaries* *that may switch within an interevent interval. Such within-interval switching can be described by a more general switching process, such as a Markov jump process with a bounded switching rate; this extension is left for future work.*

2.3. Bounds on the deception map

To characterize how deception influences the closed-loop behavior, we assume that the falsification map $\varphi(\cdot)$ does not amplify the measurement signal in an unbounded manner. Let $v(0,t)$ denote the true values of the boundary state at $x = 0$. In particular, we impose a relative growth bound of the form.

Assumption 3. *The deception function $\varphi : \mathbb{R} \to \mathbb{R}$ is continuously differentiable and satisfies $\varphi(0) = 0$. Moreover, there exists a non-negative constant L_φ such that*

$$|\varphi(z)| \leq L_\varphi |z|, \qquad \forall z \in \mathbb{R}. \tag{2.11}$$

Remark 3. *Assumption 3 provides a tractable bound on the attack-induced deviation in terms of the genuine boundary signal. This relation is essential for the subsequent stability analysis, as it allows the deception-related terms in the observer error dynamics to be estimated in terms of the boundary and gradient energy quantities and handled using the trace and Young inequalities. Moreover, the assumption does not require $\varphi(\cdot)$ to be linear and therefore still accommodates a class of amplitude-scaling and state-dependent nonlinear distortions which satisfy the prescribed relative bound. The imposed regularity conditions ensure that the boundary trace operators appearing in the Lyapunov analysis are well-defined and that the corresponding boundary terms can be bounded by the energy norms.*

2.4. Observer construction and estimation error dynamics

Let $\hat{v}(x,t)$ represent the observer state driven by the attacked boundary measurement $y_r(t)$. We consider the following output-injection observer:

$$\hat{v}_t(x,t) = \varepsilon\hat{v}_{xx}(x,t) + \lambda\hat{v}(x,t) + p_1(x)(y_r(t) - \hat{v}(0,t)), \tag{2.12}$$

$$\hat{v}_x(0,t) = p_{10}(y_r(t) - \hat{v}(0,t)), \tag{2.13}$$

$$\hat{v}_x(1,t) + q\hat{v}(1,t) = U(t) \tag{2.14}$$

with the initial condition

$$\hat{v}(x,0) = \hat{v}_0(x), \qquad x \in (0,1).$$

Here, $p_1(x)$ and p_{10} denote the observer gains, which are determined by the subsequent backstepping design, and $U(t)$ denotes the boundary actuation. Define the estimation error variable

$$\tilde{v}(x,t) = v(x,t) - \hat{v}(x,t) \tag{2.15}$$

based on (2.1)–(2.3) and (2.12)–(2.14), and utilizing (2.7) and (2.8), one obtains the error dynamics

$$\begin{aligned}\tilde{v}_t(x,t) = {}& \varepsilon\tilde{v}_{xx}(x,t) + \lambda\tilde{v}(x,t) - p_1(x)\Big(\beta(t)\tilde{v}(0,t) \\ & + (1-\beta(t))(\varphi(v(0,t)) - \hat{v}(0,t))\Big),\end{aligned} \tag{2.16}$$

$$\tilde{v}_x(0,t) = -p_{10}\Big(\beta(t)\tilde{v}(0,t) + (1-\beta(t))(\varphi(v(0,t)) - \hat{v}(0,t))\Big), \tag{2.17}$$

$$\tilde{v}_x(1,t) + q\tilde{v}(1,t) = 0. \tag{2.18}$$

Remark 4. *In the nominal case (no attack), namely when $\beta(t) \equiv 1$, then $y_r(t) = y_b(t) = v(0,t)$. Then,* (2.16)–(2.18) *reduce to the standard backstepping observer error system, where the correction terms depend solely on the true boundary measurement. Under deceptive measurements ($\beta(t) = 0$ on certain intervals), additional terms involving $\varphi(\cdot)$ enter the injection channel. Importantly, the diffusion–reaction operator in the error PDE is unchanged; the attack affects the error system only through the measurement-driven injection at the boundary and in the distributed correction term. Accordingly, the attack-induced contribution is retained explicitly in the estimation error dynamics and is subsequently collected into the measurement deviation $\Delta_y(t)$ in Section 3, where it is treated as a disturbance input of the transformed error system.*

2.5. Technical tools and auxiliary estimates

In this subsection, we recall several classical estimates that will be repeatedly used in the subsequent backstepping design and Lyapunov analysis.

Lemma 1 (One-dimensional trace inequality [35])**.** *There exists a constant $C > 0$ such that for every $z(\cdot,t) \in H^1(0,1)$,*

$$|z(1,t)|^2 \leq C(\|z[t]\|^2 + \|z_x[t]\|^2).$$

This inequality is a consequence of the continuity of the trace mapping from $H^1(0,1)$ into $\mathbb{R}$, and it will be used to estimate boundary terms in the Lyapunov analysis.

Lemma 2 (Cauchy–Schwarz inequality [36])**.** *For each fixed $t \geq 0$, any $f(\cdot,t)$, $g(\cdot,t) \in L^2(0,1)$ satisfy*

$$\left|\int_0^1 f(x,t)\, g(x,t)\, dx\right| \leq \left(\int_0^1 f^2(x,t)\, dx\right)^{1/2} \left(\int_0^1 g^2(x,t)\, dx\right)^{1/2}.$$

Equivalently,

$$\left|\int_0^1 f(x,t)\, g(x,t)\, dx\right| \leq \|f(\cdot,t)\|_{L^2(0,1)}\, \|g(\cdot,t)\|_{L^2(0,1)}.$$

This inequality will be used to bound inner product terms in the Lyapunov derivative estimates and in the input-to-state stability (ISS) analysis.

Lemma 3 (Young's inequality [36])**.** *For any $a, b \in \mathbb{R}$ and any $\delta > 0$,*

$$ab \leq \frac{\delta}{2}a^2 + \frac{1}{2\delta}b^2.$$

This inequality will be repeatedly used to balance cross terms arising in the Lyapunov derivative estimates.

Lemma 4 (ISS differential inequality [37, 38])**.** *Assume that $V : [0,\infty) \to [0,\infty)$ is locally absolutely continuous and that $w \in L^2_{\mathrm{loc}}([0,\infty))$. Suppose that for some constants $\alpha > 0$ and $\gamma > 0$,*

$$\dot{V}(t) \leq -\alpha V(t) + \gamma w^2(t)$$

holds for almost every $t \geq 0$. Then,

$$V(t) \leq e^{-\alpha t} V(0) + \gamma \int_0^t e^{-\alpha(t-s)} w^2(s)\, ds, \qquad t \geq 0.$$

In particular:

- *If* $w(t) \equiv 0$*, then* $V(t) \le e^{-\alpha t} V(0)$*, and exponential stability holds.*
- *If* $w(t) \in L_\infty[0,\infty)$*, then* $V(t)$ *stays bounded on* $[0,\infty)$*.*

When deceptive measurements are taken into account, the transformed error dynamics cannot be treated as a purely autonomous stable system because the attack effect enters the PDE through the measurement deviation $\Delta_y(t)$ and acts as a disturbance input in both the distributed and boundary channels. Hence, the appropriate stability notion is no longer merely exponential convergence of the zero solution but should instead be formulated in the ISS sense with reference to the interference $\Delta_y(t)$. This viewpoint is consistent with the later Lyapunov estimate, where the derivative of the energy functional takes the form of an ISS differential inequality. In particular, the ISS framework enables us to show that bounded attack inputs produce bounded estimation errors and that the nominal exponential convergence is recovered when the attack input vanishes.

Lemma 5 (Robin–Poincaré inequality [39])**.** *Let* $q > 1/2$*. Then, for any* $z(\cdot,t) \in H^1(0,1)$ *and each fixed* $t \ge 0$*,*

$$\int_0^1 z_x^2(x,t)\,dx + qz^2(1,t) \ge \theta \int_0^1 z^2(x,t)\,dx, \qquad \theta := \min\left\{q - \frac{1}{2}, \frac{1}{2}\right\}.$$

This inequality follows from the spectral properties of the one-dimensional Sturm–Liouville operator associated with the Robin boundary condition. It guarantees that the boundary dissipation contributes a strictly positive coercive margin in the energy estimate.

3. Backstepping transformations

Because both the observer error system and the plant dynamics are governed by reaction–diffusion equations with boundary measurements and boundary actuation, direct stability analysis is complicated by the presence of unbounded boundary operators and the coupling between distributed states and boundary terms. The backstepping approach provides a systematic way to overcome this difficulty: By constructing suitable Volterra integral transformations, the original systems can be converted into target systems with simpler boundary structures and more tractable dissipative properties, which lays the foundation for the subsequent Lyapunov analysis and event-triggered design. In the present attacked setting, backstepping also plays an essential role in isolating the effect of deceptive measurements into explicit perturbation terms driven by the measurement deviation $\Delta_y(t)$, thereby making the attack influence amenable to a structured stability analysis.

For the considered one-dimensional reaction–diffusion system, the Volterra transformation is particularly suitable because its triangular integral structure, $0 \le \xi \le x \le 1$, is naturally consistent with the ordered spatial domain and with the triangular kernel domain used in the backstepping design. This structure enables the distributed reaction dynamics and boundary couplings to be handled systematically through the associated kernel equations.

This section is carried out in two steps. We first consider the nominal case without deceptive attacks [29], in which the backstepping transformation is designed so that the observer error system is transformed into a target PDE with an exponentially stable structure. We then consider the attacked case, where the same backstepping design is retained, but the deception effect is represented explicitly through distributed and left-boundary perturbation terms. This two-step presentation distinguishes the nominal stabilizing mechanism from the additional disturbance effects induced by deceptive measurements and prepares the subsequent ISS and mean-square stability analyses.

Following the observer error backstepping construction in [29], we employ the Volterra transformation

$$\tilde{v}(x,t) = \tilde{z}(x,t) - \int_0^x P(x,\xi)\tilde{z}(\xi,t)\,d\xi, \tag{3.1}$$

whose inverse is

$$\tilde{z}(x,t) = \tilde{v}(x,t) + \int_0^x Q(x,\xi)\tilde{v}(\xi,t)\,d\xi, \tag{3.2}$$

where $P(x,\xi)$ and $Q(x,\xi)$ denote the backstepping kernel and its inverse kernel, respectively. The kernel $P(x,y)$ is determined by the following boundary value problem posed on the triangular area $\{(x,y) : 0 \le y \le x \le 1\}$ [29]:

$$P_{xx}(x,y) - P_{yy}(x,y) = -\frac{\lambda}{\varepsilon}P(x,y), \qquad 0 \le y \le x \le 1, \tag{3.3}$$

$$P_x(1,y) = -qP(1,y), \qquad 0 \le y \le 1, \tag{3.4}$$

$$P(x,x) = \frac{\lambda}{2\varepsilon}(x-1), \qquad 0 \le x \le 1. \tag{3.5}$$

By Assumption 1, the boundary value problem (3.3)–(3.5) admits a unique Volterra kernel solution P. Moreover, by standard Volterra theory for backstepping transformations, the inverse kernel Q exists and is bounded, and hence, the mapping (3.1)–(3.2) is boundedly invertible in $L^2(0,1)$.

If no deceptive attack occurs, substituting (3.1) into the nominal error system (2.16)–(2.18) (with $\beta(t) \equiv 1$ so that $y_r(t) = v(0,t)$) and using (3.3)–(3.5) yields the nominal target error system in [29]:

$$\tilde{z}_t(x,t) = \varepsilon\tilde{z}_{xx}(x,t), \tag{3.6}$$

$$\tilde{z}_x(0,t) = 0, \tag{3.7}$$

$$\tilde{z}_x(1,t) = -q\tilde{z}(1,t). \tag{3.8}$$

The corresponding observer gains are

$$p_1(x) = \varepsilon P_y(x,0), \qquad p_{10} = P(0,0) = -\frac{\lambda}{2\varepsilon}. \tag{3.9}$$

Here, the relation for $p_1(x)$ follows from the backstepping coefficient matching, and the last equality for p_{10} follows directly from (3.5) evaluated at $x = 0$.

When deceptive measurements are present, it is useful to distinguish the nominal observer innovation from the perturbation caused solely by measurement falsification. To this end, we define the attack-induced measurement deviation as

$$\Delta_y(t) = y_r(t) - y_b(t) = (1-\beta(t))\left[\varphi(v(0,t)) - v(0,t)\right]. \tag{3.10}$$

Accordingly,

$$y_r(t) - \hat{v}(0,t) = \tilde{v}(0,t) + \Delta_y(t).$$

In the attack-free case, that is, when $\beta(t) \equiv 1$, one has $\Delta_y(t) \equiv 0$.

Using $y_r(t) - \hat{v}(0,t) = \tilde{v}(0,t) + \Delta_y(t)$, the estimation error system (2.16)–(2.18) can be equivalently rewritten as

$$\begin{aligned}\tilde{v}_t(x,t) &= \varepsilon\tilde{v}_{xx}(x,t) + \lambda\tilde{v}(x,t) - p_1(x)\tilde{v}(0,t) - p_1(x)\Delta_y(t),\\ \tilde{v}_x(0,t) &= -p_{10}\tilde{v}(0,t) - p_{10}\Delta_y(t),\\ \tilde{v}_x(1,t) + q\tilde{v}(1,t) &= 0.\end{aligned}$$

Applying the inverse Volterra transformation (3.2) to the above equivalent error system and using the kernel identities induced by the mutually inverse transformations (3.1)–(3.2) together with the observer gain relations in (3.9) yields

$$\tilde{z}_t(x,t) = \varepsilon\tilde{z}_{xx}(x,t) + f_a(x,t), \tag{3.11}$$

$$\tilde{z}_x(0,t) = b_0\Delta_y(t), \tag{3.12}$$

$$\tilde{z}_x(1,t) = -q\tilde{z}(1,t). \tag{3.13}$$

At $x = 0$, the forward transformation (3.1) gives $\tilde{v}(0,t) = \tilde{z}(0,t)$ and

$$\tilde{v}_x(0,t) = \tilde{z}_x(0,t) - P(0,0)\tilde{z}(0,t).$$

Using $P(0,0) = p_{10}$ together with the left-boundary condition of the equivalent error system yields

$$\tilde{z}_x(0,t) = -p_{10}\Delta_y(t).$$

Hence,

$$b_0 = -p_{10}.$$

Furthermore,

$$f_a(x,t) = b(x)\Delta_y(t), \qquad b(x) = -p_1(x) - \int_0^x Q(x,\xi)p_1(\xi)\,d\xi + \varepsilon p_{10}Q(x,0). \tag{3.14}$$

Because Q, p_1, and p_{10} are bounded, $b(\cdot)$ is bounded on $[0,1]$.

Remark 5. *The definition of* $\Delta_y(t)$ *in* (3.10) *separates the deception-induced measurement deviation from the nominal observer innovation. In particular,* $\beta(t) \equiv 1$ *implies* $\Delta_y(t) \equiv 0$*. The attack affects the estimation error dynamics through the distributed observer injection and the boundary injection at* $x = 0$*, whereas the original estimation error condition at* $x = 1$ *remains homogeneous.*

Indeed, differentiating (3.1) *with respect to x and evaluating it at* $x = 1$ *gives*

$$\tilde{v}_x(1,t) + q\tilde{v}(1,t) = \tilde{z}_x(1,t) + q\tilde{z}(1,t) - P(1,1)\tilde{z}(1,t) - \int_0^1 [P_x(1,\xi) + qP(1,\xi)]\tilde{z}(\xi,t)\,d\xi.$$

Because $P(1,1) = 0$ *follows from* (3.5)*, and* $P_x(1,\xi) = -qP(1,\xi)$ *follows from* (3.4)*, the last two terms vanish. Together with* $\tilde{v}_x(1,t) + q\tilde{v}(1,t) = 0$*, this yields*

$$\tilde{z}_x(1,t) = -q\tilde{z}(1,t).$$

Therefore, in the transformed coordinates, the deception effect appears through the distributed term $b(x)\Delta_y(t)$ *and the left-boundary perturbation* $b_0\Delta_y(t)$*, and no additional attack-induced term arises at the right boundary.*

Proposition 1. *Under the standing regularity assumptions, if $\Delta_y(t) \equiv 0$, the transformed observer error system* (3.11)–(3.13) *with f_a defined by* (3.14) *reduces to the nominal target system and is globally exponentially stable in $L^2(0,1)$. Moreover, for bounded attack-induced measurement deviations $\Delta_y(t)$ satisfying the standing regularity assumptions, the perturbed transformed observer error system is input-to-state stable with respect to $\Delta_y(t)$. In particular, in the attack-free case, that is, $\beta(t) \equiv 1$, one has $\Delta_y(t) \equiv 0$, and hence, the observer error $\tilde{v}(\cdot,t)$ converges exponentially to zero in $L^2(0,1)$. Under bounded deceptive measurement deviations, the observer error remains bounded according to the corresponding ISS estimate.*

Proof. We first consider $\Delta_y(t) \equiv 0$, for which (3.11)–(3.13) reduce to the nominal target error system. Define the Lyapunov functional

$$V(t) = \frac{1}{2}\int_0^1 \tilde{z}^2(x,t)\,dx.$$

Differentiating with respect to time yields

$$\dot{V}(t) = \int_0^1 \tilde{z}(x,t)\,\tilde{z}_t(x,t)\,dx.$$

Substituting the target error system (3.6),

$$\dot{V}(t) = \varepsilon\int_0^1 \tilde{z}(x,t)\,\tilde{z}_{xx}(x,t)\,dx.$$

Integrating by parts with respect to x yields

$$\dot{V}(t) = \varepsilon\Big[\tilde{z}(x,t)\tilde{z}_x(x,t)\Big]_0^1 - \varepsilon\int_0^1 \tilde{z}_x^2(x,t)\,dx.$$

From $\tilde{z}_x(0,t) = 0$ and $\tilde{z}_x(1,t) = -q\tilde{z}(1,t)$, this yields

$$\dot{V}(t) = -\varepsilon\int_0^1 \tilde{z}_x^2(x,t)\,dx - \varepsilon q\tilde{z}^2(1,t) \le 0.$$

For every $\tilde{z}(\cdot,t) \in H^1(0,1)$, we have

$$\|\tilde{z}[t]\|^2 \le 2\left(\|\tilde{z}_x[t]\|^2 + |\tilde{z}(1,t)|^2\right).$$

Hence, by defining

$$\theta_q := \frac{1}{2}\min\{1,q\} > 0,$$

we obtain

$$\|\tilde{z}_x[t]\|^2 + q|\tilde{z}(1,t)|^2 \ge \theta_q\|\tilde{z}[t]\|^2.$$

Therefore,

$$\dot{V}(t) \le -\varepsilon\theta_q\|\tilde{z}[t]\|^2 = -2\varepsilon\theta_q V(t),$$

and consequently,

$$V(t) \le e^{-2\varepsilon\theta_q t}V(0).$$

Equivalently,

$$\|\tilde{z}[t]\| \le e^{-\varepsilon\theta_q t}\|\tilde{z}[0]\|.$$

Because the Volterra transformations (3.1)–(3.2) are bounded and invertible in $L^2(0,1)$, there exist constants $M_1, M_2 > 0$ such that

$$\|\tilde{v}[t]\| \le M_1\|\tilde{z}[t]\|, \qquad \|\tilde{z}[0]\| \le M_2\|\tilde{v}[0]\|.$$

Therefore,

$$\|\tilde{v}[t]\| \le M_1 M_2 e^{-\varepsilon\theta_q t}\|\tilde{v}[0]\|,$$

which establishes exponential convergence of the observer error in the nominal case.

We now consider the perturbed system under a bounded attack-induced measurement deviation $\Delta_y(t)$. From (3.11)–(3.14), the transformed observer error system satisfies

$$\begin{aligned} \tilde{z}_t(x,t) &= \varepsilon\tilde{z}_{xx}(x,t) + b(x)\Delta_y(t), \\ \tilde{z}_x(0,t) &= b_0\Delta_y(t), \\ \tilde{z}_x(1,t) &= -q\tilde{z}(1,t). \end{aligned}$$

Consider the Lyapunov functional

$$V(t) = \frac{1}{2}\int_0^1 \tilde{z}^2(x,t)\,dx.$$

For almost every t on each interevent interval, differentiating along the solutions and integrating by parts yields

$$\dot{V}(t) = -\varepsilon\|\tilde{z}_x[t]\|^2 - \varepsilon q|\tilde{z}(1,t)|^2 - \varepsilon b_0\Delta_y(t)\tilde{z}(0,t) + \Delta_y(t)\int_0^1 b(x)\tilde{z}(x,t)\,dx.$$

Define

$$D_q(t) := \|\tilde{z}_x[t]\|^2 + q|\tilde{z}(1,t)|^2.$$

For every $\tilde{z}(\cdot,t) \in H^1(0,1)$,

$$\|\tilde{z}[t]\|^2 \le 2\left(\|\tilde{z}_x[t]\|^2 + |\tilde{z}(1,t)|^2\right).$$

Consequently,

$$D_q(t) \ge \theta_q\|\tilde{z}[t]\|^2, \qquad \theta_q := \frac{1}{2}\min\{1,q\} > 0.$$

Moreover,

$$|\tilde{z}(0,t)|^2 \le 2\left(|\tilde{z}(1,t)|^2 + \|\tilde{z}_x[t]\|^2\right) \le C_q D_q(t), \qquad C_q := 2\max\{1,q^{-1}\}.$$

For arbitrary $\eta_0 > 0$, Young's inequality gives

$$\varepsilon|b_0||\Delta_y(t)|\,|\tilde{z}(0,t)| \le \varepsilon|b_0|\sqrt{C_q}|\Delta_y(t)|\sqrt{D_q(t)} \le \eta_0 D_q(t) + \frac{\varepsilon^2 b_0^2 C_q}{4\eta_0}|\Delta_y(t)|^2.$$

Similarly, for arbitrary $\eta_1 > 0$,

$$\left|\Delta_y(t)\int_0^1 b(x)\tilde{z}(x,t)\,dx\right| \le \|b\|_{L^2(0,1)}\,|\Delta_y(t)|\,\|\tilde{z}[t]\| \le \frac{\|b\|_{L^2(0,1)}}{\sqrt{\theta_q}}|\Delta_y(t)|\sqrt{D_q(t)} \le \eta_1 D_q(t) + \frac{\|b\|^2_{L^2(0,1)}}{4\eta_1\theta_q}|\Delta_y(t)|^2.$$

Hence,

$$\dot{V}(t) \le -(\varepsilon - \eta_0 - \eta_1)D_q(t) + C_e|\Delta_y(t)|^2, \qquad C_e := \frac{\varepsilon^2 b_0^2 C_q}{4\eta_0} + \frac{\|b\|^2_{L^2(0,1)}}{4\eta_1\theta_q}.$$

Choosing $\eta_0, \eta_1 > 0$ such that $\eta_0 + \eta_1 < \varepsilon$ gives

$$\dot{V}(t) \le -\lambda_e V(t) + C_e|\Delta_y(t)|^2, \tag{3.15}$$

where

$$\lambda_e := 2\theta_q(\varepsilon - \eta_0 - \eta_1) > 0.$$

Applying Lemma 4 to (3.15) yields

$$V(t) \le e^{-\lambda_e t}V(0) + C_e \int_0^t e^{-\lambda_e(t-s)}|\Delta_y(s)|^2\, ds,$$

and therefore,

$$V(t) \le e^{-\lambda_e t}V(0) + \frac{C_e}{\lambda_e} \sup_{0\le s\le t} |\Delta_y(s)|^2.$$

Consequently,

$$\|\tilde{z}[t]\| \le e^{-\lambda_e t/2}\|\tilde{z}[0]\| + \sqrt{\frac{2C_e}{\lambda_e}} \sup_{0\le s\le t} |\Delta_y(s)|.$$

Using again the bounded invertibility of (3.1)–(3.2), we obtain

$$\|\tilde{v}[t]\| \le M_1 M_2 e^{-\lambda_e t/2}\|\tilde{v}[0]\| + M_1 \sqrt{\frac{2C_e}{\lambda_e}} \sup_{0\le s\le t} |\Delta_y(s)|.$$

Hence, the observer error system is ISS with respect to the attack-induced measurement deviation $\Delta_y(t)$. □

Remark 6. *The Volterra kernel P and the observer gains in* (3.9) *are designed from the attack-free observer error system and are not redesigned when deceptive measurements occur. With the attack-induced deviation* $\Delta_y(t)$ *defined in* (3.10)*, the transformed attack effect appears as the additive distributed disturbance* $b(x)\Delta_y(t)$ *and the left-boundary perturbation* $b_0\Delta_y(t)$*, whereas the right-boundary condition remains homogeneous. Because* $b(\cdot)$ *and* b_0 *are bounded, the deception effect can be handled at the analysis stage through the ISS estimate established in Proposition 1.*

4. Event-triggered boundary control

4.1. Backstepping for the observer and control law

To realize observer-based boundary stabilization, the estimated state $\hat{v}(\cdot, t)$ generated by the boundary observer (2.12)–(2.14) is used to construct the boundary feedback input. Guided by the backstepping framework for boundary stabilization of parabolic PDEs in [29], we introduce the Volterra transformation

$$\hat{z}(x,t) = \hat{v}(x,t) - \int_0^x K(x,\xi)\hat{v}(\xi,t)\, d\xi, \tag{4.1}$$

where the kernel $K(x, y)$ is defined on the triangular domain $0 \leq y \leq x \leq 1$ and satisfies

$$K_{xx}(x, y) - K_{yy}(x, y) = \frac{\lambda}{\varepsilon} K(x, y), \qquad 0 \leq y \leq x \leq 1, \tag{4.2}$$

$$K_y(x, 0) = 0, \qquad 0 \leq x \leq 1, \tag{4.3}$$

$$K(x, x) = -\frac{\lambda}{2\varepsilon} x, \qquad 0 \leq x \leq 1. \tag{4.4}$$

Define the parameter

$$r = q - \frac{\lambda}{2\varepsilon}. \tag{4.5}$$

Under Assumption 1, the kernel problem (4.2)–(4.4) admits a unique bounded solution K, and the corresponding inverse Volterra transformation is well-defined and bounded. Therefore, the transformation (4.1) is boundedly invertible in $L^2(0, 1)$. Denoting the corresponding inverse kernel by L, the inverse transformation can be written as

$$\hat{v}(x, t) = \hat{z}(x, t) + \int_0^x L(x, \xi)\hat{z}(\xi, t)\, d\xi.$$

By Assumption 1, one has $r > 1/2$, which provides the coercive boundary dissipation used in the subsequent stability analysis.

Define the ideal continuous-time boundary feedback signal as

$$U_c(t) = \int_0^1 \left[rK(1, y) + K_x(1, y) \right] \hat{v}(y, t)\, dy, \tag{4.6}$$

where $U_c(t)$ denotes the boundary input that would be generated continuously from the current observer state. Using

$$y_r(t) - \hat{v}(0, t) = \tilde{z}(0, t) + \Delta_y(t)$$

and applying the backstepping transformation (4.1) to the observer system (2.12)–(2.14), we obtain the following transformed observer dynamics:

$$\hat{z}_t(x, t) = \varepsilon \hat{z}_{xx}(x, t) + g(x)[\tilde{z}(0, t) + \Delta_y(t)], \tag{4.7}$$

$$\hat{z}_x(0, t) = -\frac{\lambda}{2\varepsilon}[\tilde{z}(0, t) + \Delta_y(t)], \tag{4.8}$$

$$\hat{z}_x(1, t) + r\hat{z}(1, t) = U(t) - U_c(t), \tag{4.9}$$

where

$$g(x) = p_1(x) - \frac{\lambda}{2} K(x, 0) - \int_0^x K(x, \xi) p_1(\xi)\, d\xi. \tag{4.10}$$

To verify the right-boundary relation in (4.9), differentiating (4.1) with respect to x and evaluating it at $x = 1$ gives

$$\hat{z}_x(1, t) = \hat{v}_x(1, t) - K(1, 1)\hat{v}(1, t) - \int_0^1 K_x(1, \xi)\hat{v}(\xi, t)\, d\xi.$$

Using the observer boundary condition $\hat{v}_x(1,t) = U(t) - q\hat{v}(1,t)$ together with $K(1,1) = -\lambda/(2\varepsilon)$ and $r = q - \lambda/(2\varepsilon)$, we obtain

$$\hat{z}_x(1,t) = U(t) - r\hat{v}(1,t) - \int_0^1 K_x(1,\xi)\hat{v}(\xi,t)\,d\xi.$$

Combining the above relation and (4.6) with (4.1) evaluated at $x = 1$ yields

$$\hat{z}_x(1,t) + r\hat{z}(1,t) = U(t) - U_c(t),$$

which verifies (4.9). In particular, under the ideal continuous-time implementation $U(t) = U_c(t)$, the right-boundary condition reduces to

$$\hat{z}_x(1,t) = -r\hat{z}(1,t).$$

4.2. *Input holding error*

Section 4.1 defines the ideal continuous-time boundary feedback signal $U_c(t)$ computed from the current observer state. To reduce the frequency of boundary updates, we implement this signal through an event-triggered sample-and-hold mechanism.

At each event time t_k, the controller samples the observer profile $\hat{v}(\cdot,t_k)$ and computes the corresponding ideal control value,

$$U_k = U_c(t_k) = \int_0^1 \left(rK(1,\xi) + K_x(1,\xi)\right)\hat{v}(\xi,t_k)\,d\xi. \tag{4.11}$$

The actual boundary input is achieved through a sample-and-hold strategy:

$$U(t) = U_k, \quad t \in [t_k, t_{k+1}). \tag{4.12}$$

To quantify the discrepancy between the ideal continuous-time signal $U_c(t)$ and its event-triggered implementation $U(t)$, we define the input-holding error

$$e_U(t) = U_c(t) - U(t), \quad t \in [t_k, t_{k+1}). \tag{4.13}$$

Combining (4.9) with the definition (4.13) gives

$$\hat{z}_x(1,t) = -r\hat{z}(1,t) - e_U(t), \qquad t \in [t_k, t_{k+1}). \tag{4.14}$$

Hence, under the event-triggered sample-and-hold implementation, the transformed observer dynamics are governed by (4.7), (4.8), and (4.14). The measurement deception deviation $\Delta_y(t)$ enters the distributed and left-boundary channels, whereas the input-holding error $e_U(t)$ enters the right boundary through the sample-and-hold implementation.

Under the right-continuous sample-and-hold convention, $U(t_k) = U_k = U_c(t_k)$, and hence, $e_U(t_k) = 0$ immediately after each update. Between two successive events, $e_U(t)$ generally becomes nonzero because $U(t)$ is held constant, whereas $U_c(t)$ evolves with the observer state.

4.3. Dynamic event triggering strategy

To avoid continuous updating of the control signal, we realize the boundary feedback law through an event-triggered sample-and-hold implementation. For the triggering rule, we follow the dynamic event-triggering framework in [29] for reaction–diffusion PDE boundary control: The input-holding error is monitored against a time-varying threshold for which the exclusion of Zeno behavior and a uniform positive lower bound on the interevent times will be established below.

The main difference in our setting is that the boundary sensing signal can be randomly falsified by deceptive attacks. Accordingly, we develop the closed-loop analysis in Section 5 in the mean-square sense, explicitly accounting for the attack-induced stochasticity in the observer dynamics and coupling the triggering variable with the estimation energy terms required in the attacked case.

Let $\{t_k\}_{k\in\mathbb{N}}$ denote the event sequence, where $0 = t_0 < t_1 < t_2 < \cdots$. On each interevent interval $t \in [t_k, t_{k+1})$, the boundary input is held at $U(t) = U_k = U_c(t_k)$, and the input-holding error $e_U(t)$ is given by (4.13) and satisfies $e_U(t_k) = 0$.

Define the next event time

$$t_{k+1} = \inf\left\{t > t_k : e_U^2(t^-) \geq -\kappa\zeta(t)\right\}. \tag{4.15}$$

Here, $e_U(t^-)$ denotes the input-holding error immediately before a possible control update. On each open interevent interval, $e_U(t^-) = e_U(t)$, whereas at a triggering instant, the left-limit notation distinguishes the pre-update triggering value from the post-update reset of the holding error. More precisely, the evolution of $\zeta(t)$ modulates the dynamic triggering threshold in real time and is instrumental in ruling out Zeno behavior. The variable $\zeta(t)$ satisfies

$$\dot{\zeta}(t) = -a_\zeta\zeta(t) + b_\zeta e_U^2(t) - c_1\,\|\hat{z}_x[t]\|^2 - c_2|\hat{z}(1,t)|^2 - c_3|\tilde{z}(0,t)|^2, \tag{4.16}$$

where $a_\zeta, b_\zeta, c_1, c_2, c_3 > 0$ are design parameters, and $\|f[t]\| := \|f(\cdot,t)\|_{L^2(0,1)}$. The internal variable $\zeta(t)$ is not reset at triggering instants and therefore remains continuous across control updates.

The deception considered in this paper acts on the boundary measurement channel $y_b \mapsto y_r$ used for observer correction. Under the adopted information structure, the event generator is assumed to have access to the local boundary estimation mismatch $\tilde{v}(0,t)$ required by (4.16) together with the observer variables entering the triggering mechanism. Because the Volterra transformation for the estimation error reduces to the identity at $x = 0$, one has $\tilde{z}(0,t) = \tilde{v}(0,t)$. This information availability assumption is part of the adopted control architecture and is not inferred from the potentially falsified observer measurement $y_r(t)$. Accordingly, attacks affecting the signals available internally to the event generator are outside the scope of the present model.

Because $\zeta(t) < 0$, the quantity $-\kappa\zeta(t)$ defines a positive dynamic triggering threshold. For a fixed value of $\zeta(t)$, a larger κ increases this threshold and therefore tends to allow a larger input-holding error before a new event is generated. The term $-a_\zeta\zeta(t)$ drives $\zeta(t)$ toward zero and thus tends to decrease the positive threshold, whereas $b_\zeta e_U^2(t)$ strengthens this effect as the input-holding error grows, making a new control update more likely. The parameters c_1, c_2, and c_3 weight the contributions of the observer state gradient energy $\|\hat{z}_x[t]\|^2$, the boundary value $|\hat{z}(1,t)|^2$, and the boundary estimation mismatch $|\tilde{z}(0,t)|^2$, respectively. These terms drive $\zeta(t)$ toward more negative values and thereby enlarge the dynamic threshold according to the corresponding closed-loop energy levels. Hence, these parameters provide additional flexibility in balancing the control update frequency and closed-loop performance. Because the threshold and the closed-loop states are dynamically coupled, these effects should be understood qualitatively rather than as strict monotonic relationships. In practice, the triggering parameters are selected jointly so that the sufficient conditions for closed-loop stability and Zeno-free behavior established in the subsequent analysis are satisfied.

Compared with conventional static event-triggered schemes, in which the triggering threshold is prescribed directly by instantaneous closed-loop quantities, the proposed mechanism introduces $\zeta(t)$ as an internal dynamic variable. Consequently, the threshold $-\kappa\zeta(t)$ evolves with the closed-loop dynamics, providing an additional degree of freedom to adjust the triggering sensitivity over time and thereby offering greater flexibility in balancing closed-loop performance and the frequency of control updates.

We choose the initial condition $\zeta(t_0) = \zeta_0 < 0$. Under the regularity conditions stated in Section 2, the forcing terms in (4.16) are locally integrable on each interevent interval, and hence, $\zeta(t)$ admits a unique absolutely continuous solution for the given closed-loop trajectory. Together, (4.15)–(4.16) define a fully dynamic event-triggering scheme. As shown in Lemma 6, the negativity of $\zeta(t)$ is preserved for all $t \geq t_0$, and the additional parameter conditions ensuring a uniform positive lower bound on the interevent times are given in Theorem 1.

4.4. Triggering inequality and negativity of $\zeta(t)$

Lemma 6 (Triggering inequality and negativity of $\zeta(t)$)**.** *Suppose $\zeta(0) < 0$, and $\kappa, a_\zeta, b_\zeta, c_1, c_2, c_3 > 0$. Then, for each interevent interval $[t_k, t_{k+1})$,*

$$e_U^2(t) < -\kappa\zeta(t), \qquad \zeta(t) < 0, \qquad t \in [t_k, t_{k+1}). \tag{4.17}$$

Moreover, $\zeta(t) < 0$ for all $t \geq 0$. If $t_{k+1} < \infty$, the pre-update holding error satisfies

$$e_U^2(t_{k+1}^-) = -\kappa\zeta(t_{k+1}), \tag{4.18}$$

whereas the subsequent control update resets the actual input-holding error to $e_U(t_{k+1}) = 0$.

Proof. We argue on each interevent interval and then conclude by induction. Between two events, $U(t)$ is held constant, and $\zeta(t)$ evolves according to the ordinary differential equation (ODE) (4.16). Under the regularity conditions stated in Section 2, the right-hand side of (4.16) is locally integrable along the closed-loop trajectory on each interevent interval. Hence, $\zeta(\cdot)$ is absolutely continuous, and therefore continuous, on $[t_k, t_{k+1})$. Moreover, $e_U(t) = U_c(t) - U(t)$ is also continuous on $[t_k, t_{k+1})$ because $U(t) = U_c(t_k)$ on this interval. The triggering instant is determined by (4.15):

$$t_{k+1} = \inf\left\{t > t_k : e_U^2(t^-) \geq -\kappa\zeta(t)\right\}.$$

At $t = t_k$, the post-update value satisfies $e_U(t_k) = 0$. Hence, whenever $\zeta(t_k) < 0$,

$$e_U^2(t_k) = 0 < -\kappa\zeta(t_k).$$

Now, take any $t \in (t_k, t_{k+1})$. Because no control update occurs inside the open interevent interval, $e_U(t^-) = e_U(t)$. If $e_U^2(t) \geq -\kappa\zeta(t)$ held at such a time, then, equivalently, $e_U^2(t^-) \geq -\kappa\zeta(t)$, and the definition of t_{k+1} would imply $t_{k+1} \leq t$, contradicting $t < t_{k+1}$. Therefore,

$$e_U^2(t) < -\kappa\zeta(t), \qquad t \in [t_k, t_{k+1}).$$

Thus, the triggering inequality remains strict throughout $[t_k, t_{k+1})$. If $t_{k+1} < \infty$, continuity of the pre-update flow value of the holding error and continuity of ζ imply

$$e_U^2(t_{k+1}^-) = -\kappa\zeta(t_{k+1}).$$

After the boundary input is updated at t_{k+1}, the actual holding error is reset to $e_U(t_{k+1}) = 0$.
Using (4.16) and discarding the nonpositive terms $-c_1\|\hat{z}_x[t]\|^2 - c_2|\hat{z}(1,t)|^2 - c_3|\tilde{z}(0,t)|^2$, we have on $[t_k, t_{k+1})$

$$\dot{\zeta}(t) \le -a_\zeta\zeta(t) + b_\zeta e_U^2(t).$$

Using the relaxed bound $e_U^2(t) \le -\kappa\zeta(t)$ implied by the strict triggering inequality, we obtain

$$\dot{\zeta}(t) \le -a_\zeta\zeta(t) - b_\zeta\kappa\,\zeta(t) = -(a_\zeta + b_\zeta\kappa)\,\zeta(t).$$

Let $\vartheta := a_\zeta + b_\zeta\kappa > 0$. The differential inequality implies

$$\zeta(t) \le \zeta(t_k)e^{-\vartheta(t-t_k)}, \qquad t \in [t_k, t_{k+1}).$$

If $\zeta(t_k) < 0$, then the right-hand side remains strictly negative for $t \ge t_k$, so $\zeta(t) < 0$ on $[t_k, t_{k+1})$. If $t_{k+1} < \infty$, taking $t \to t_{k+1}^-$ and using the continuity of ζ across the triggering instant yields $\zeta(t_{k+1}) < 0$, as well. Starting from $\zeta(0) < 0$ and repeating the above argument over successive interevent intervals concludes that $\zeta(t) < 0$ for all $t \ge 0$; equivalently, the set $\{\zeta(t) < 0\}$ is forward invariant. □

4.5. Derivative of $e_U^2(t)$

Lemma 7. *Under the regularity conditions stated in Section 2, suppose that the function h defined below belongs to $H^1(0,1)$ and that $g \in L^\infty(0,1)$. Then, there exist constants $\rho_1' > 0$ and $\alpha_1', \alpha_2', \alpha_3' \ge 0$, independent of the event index k, such that for each interevent interval $[t_k, t_{k+1})$ and for almost every $t \in (t_k, t_{k+1})$,*

$$\frac{d}{dt}(e_U^2(t)) \le \rho_1' e_U^2(t) + \alpha_1'\|\hat{z}_x[t]\|^2 + \alpha_2'|\hat{z}(1,t)|^2 + \alpha_3'|\tilde{z}(0,t)|^2.$$

Proof. On each interevent interval $[t_k, t_{k+1})$, the implemented boundary input satisfies $U(t) = U_k = U_c(t_k)$ and is constant between two successive triggering instants. Therefore, the input-holding error satisfies

$$e_U(t) = U_c(t) - U(t) = U_c(t) - U_k.$$

Hence, for almost every $t \in (t_k, t_{k+1})$,

$$\dot{e}_U(t) = \dot{U}_c(t).$$

Under the right-continuous implementation convention, the held input is updated at each triggering instant so that $U(t_k) = U_c(t_k)$, and hence, $e_U(t_k) = 0$. Thus, it suffices to derive an estimate for $\dot{U}_c(t)$ on each open interevent interval. From the continuous-time boundary feedback law,

$$U_c(t) = \int_0^1 \left[rK(1,\xi) + K_x(1,\xi)\right]\hat{v}(\xi,t)\,d\xi.$$

Using the inverse backstepping transformation $\hat{v}(y,t) = \hat{z}(y,t) + \int_0^y L(y,\varrho)\hat{z}(\varrho,t)\,d\varrho$, we obtain

$$U_c(t) = \int_0^1 \left[rK(1,y) + K_x(1,y)\right]\hat{z}(y,t)\,dy + \int_0^1 \left[rK(1,y) + K_x(1,y)\right]\int_0^y L(y,\varrho)\hat{z}(\varrho,t)\,d\varrho\,dy.$$

Reversing the order of integration in the second term gives

$$\int_0^1 [rK(1,y) + K_x(1,y)] \int_0^y L(y,\varrho)\hat{z}(\varrho,t)\,d\varrho\,dy = \int_0^1 \left(\int_\varrho^1 [rK(1,y) + K_x(1,y)]\,L(y,\varrho)\,dy \right) \hat{z}(\varrho,t)\,d\varrho.$$

Hence,

$$U_c(t) = \int_0^1 h(x)\hat{z}(x,t)\,dx,$$

where

$$h(x) = rK(1,x) + K_x(1,x) + \int_x^1 [rK(1,y) + K_x(1,y)]\,L(y,x)\,dy.$$

Because $h \in H^1(0,1)$, one has $\|h_x\|_{L^2(0,1)} < \infty$, and the boundary values $h(0)$ and $h(1)$ are well-defined. For almost every $t \in (t_k, t_{k+1})$, differentiating under the integral sign yields

$$\dot{U}_c(t) = \int_0^1 h(x)\hat{z}_t(x,t)\,dx.$$

Using the transformed observer dynamics (4.7), we obtain

$$\dot{U}_c(t) = \varepsilon \int_0^1 h(x)\hat{z}_{xx}(x,t)\,dx + [\tilde{z}(0,t) + \Delta_y(t)] \int_0^1 h(x)g(x)\,dx.$$

For the diffusion term, integration by parts gives

$$\varepsilon \int_0^1 h(x)\hat{z}_{xx}(x,t)\,dx = \varepsilon h(1)\hat{z}_x(1,t) - \varepsilon h(0)\hat{z}_x(0,t) - \varepsilon \int_0^1 h_x(x)\hat{z}_x(x,t)\,dx.$$

Using (4.14) and (4.8), we obtain

$$\varepsilon \int_0^1 h(x)\hat{z}_{xx}(x,t)\,dx = -\varepsilon r h(1)\hat{z}(1,t) - \varepsilon h(1)e_U(t) + \frac{\lambda}{2}h(0)[\tilde{z}(0,t) + \Delta_y(t)] - \varepsilon \int_0^1 h_x(x)\hat{z}_x(x,t)\,dx.$$

Therefore,

$$\dot{U}_c(t) = -\varepsilon \int_0^1 h_x(x)\hat{z}_x(x,t)\,dx - \varepsilon r h(1)\hat{z}(1,t) - \varepsilon h(1)e_U(t) + \left[\frac{\lambda}{2}h(0) + \int_0^1 h(x)g(x)\,dx\right][\tilde{z}(0,t) + \Delta_y(t)].$$

Define

$$H_g := \frac{\lambda}{2}h(0) + \int_0^1 h(x)g(x)\,dx.$$

Then,

$$\dot{U}_c(t) = -\varepsilon \int_0^1 h_x(x)\hat{z}_x(x,t)\,dx - \varepsilon r h(1)\hat{z}(1,t) - \varepsilon h(1)e_U(t) + H_g[\tilde{z}(0,t) + \Delta_y(t)]. \tag{4.19}$$

We next estimate the term involving $\Delta_y(t)$. By the definition of the attack-induced measurement deviation,

$$\Delta_y(t) = (1 - \beta(t))\,[\varphi(v(0,t)) - v(0,t)]\,.$$

By Assumption 3 and taking mathematical expectation, one has

$$|\Delta_y(t)| \le (1 - P_g)(L_\varphi + 1)|v(0,t)|.$$

Moreover, $v(0,t) = \tilde{v}(0,t) + \hat{v}(0,t)$. Because both Volterra transformations reduce to the identity at $x = 0$,

$$\tilde{v}(0,t) = \tilde{z}(0,t), \qquad \hat{v}(0,t) = \hat{z}(0,t),$$

and hence,

$$v(0,t) = \tilde{z}(0,t) + \hat{z}(0,t).$$

Furthermore,

$$\hat{z}(0,t) = \hat{z}(1,t) - \int_0^1 \hat{z}_x(x,t)\,dx.$$

By the Cauchy–Schwarz inequality,

$$|\hat{z}(0,t)| \le |\hat{z}(1,t)| + \|\hat{z}_x[t]\|.$$

Consequently,

$$|\Delta_y(t)| \le (1 - P_g)(L_\varphi + 1)\left(|\tilde{z}(0,t)| + |\hat{z}(1,t)| + \|\hat{z}_x[t]\|\right).$$

It follows that

$$\left|\tilde{z}(0,t) + \Delta_y(t)\right| \le (1 - P_g)((L_\varphi + 2)|\tilde{z}(0,t)| + (L_\varphi + 1)|\hat{z}(1,t)| + (L_\varphi + 1)\|\hat{z}_x[t]\|). \tag{4.20}$$

Using (4.19), (4.20), and the Cauchy–Schwarz inequality, we obtain

$$\begin{aligned}
|\dot{U}_c(t)| &\le \varepsilon\|h_x\|_{L^2(0,1)}\|\hat{z}_x[t]\| + \varepsilon r|h(1)||\hat{z}(1,t)| + \varepsilon|h(1)||e_U(t)| + |H_g|\left|\tilde{z}(0,t) + \Delta_y(t)\right| \\
&\le \varepsilon|h(1)||e_U(t)| + \left[\varepsilon\|h_x\|_{L^2(0,1)} + (1 - P_g)(L_\varphi + 1)|H_g|\right]\|\hat{z}_x[t]\| \\
&\quad + \left[\varepsilon r|h(1)| + (1 - P_g)(L_\varphi + 1)|H_g|\right]|\hat{z}(1,t)| + (1 - P_g)(L_\varphi + 2)|H_g||\tilde{z}(0,t)|.
\end{aligned}$$

Define

$$\begin{aligned}
k_0 &:= \varepsilon|h(1)|, \\
k_1 &:= \varepsilon\|h_x\|_{L^2(0,1)} + (1 - P_g)(L_\varphi + 1)|H_g|, \\
k_2 &:= \varepsilon r|h(1)| + (1 - P_g)(L_\varphi + 1)|H_g|, \\
k_3 &:= (1 - P_g)(L_\varphi + 2)|H_g|.
\end{aligned}$$

Then,

$$|\dot{U}_c(t)| \le k_0|e_U(t)| + k_1\|\hat{z}_x[t]\| + k_2|\hat{z}(1,t)| + k_3|\tilde{z}(0,t)|.$$

Because $\dot{e}_U(t) = \dot{U}_c(t)$ for almost every $t \in (t_k, t_{k+1})$, we have

$$|\dot{e}_U(t)| \le k_0|e_U(t)| + k_1\|\hat{z}_x[t]\| + k_2|\hat{z}(1,t)| + k_3|\tilde{z}(0,t)|.$$

Therefore,

$$\frac{d}{dt}e_U^2(t) \le 2k_0 e_U^2(t) + 2k_1|e_U(t)|\|\hat{z}_x[t]\| + 2k_2|e_U(t)||\hat{z}(1,t)| + 2k_3|e_U(t)||\tilde{z}(0,t)|.$$

For arbitrary $\delta_1, \delta_2, \delta_3 > 0$, Young's inequality gives

$$2k_1|e_U(t)|\|\hat{z}_x[t]\| \le \delta_1 e_U^2(t) + \frac{k_1^2}{\delta_1}\|\hat{z}_x[t]\|^2,$$

$$2k_2|e_U(t)||\hat{z}(1,t)| \le \delta_2 e_U^2(t) + \frac{k_2^2}{\delta_2}|\hat{z}(1,t)|^2,$$

$$2k_3|e_U(t)||\tilde{z}(0,t)| \le \delta_3 e_U^2(t) + \frac{k_3^2}{\delta_3}|\tilde{z}(0,t)|^2.$$

Combining these estimates yields

$$\frac{d}{dt}e_U^2(t) \le (2k_0 + \delta_1 + \delta_2 + \delta_3)\, e_U^2(t) + \frac{k_1^2}{\delta_1}\|\hat{z}_x[t]\|^2 + \frac{k_2^2}{\delta_2}|\hat{z}(1,t)|^2 + \frac{k_3^2}{\delta_3}|\tilde{z}(0,t)|^2.$$

Finally, setting

$$\rho_1' := 2k_0 + \delta_1 + \delta_2 + \delta_3,$$

$$\alpha_1' := \frac{k_1^2}{\delta_1}, \qquad \alpha_2' := \frac{k_2^2}{\delta_2}, \qquad \alpha_3' := \frac{k_3^2}{\delta_3},$$

one has

$$\frac{d}{dt}e_U^2(t) \le \rho_1' e_U^2(t) + \alpha_1'\|\hat{z}_x[t]\|^2 + \alpha_2'|\hat{z}(1,t)|^2 + \alpha_3'|\tilde{z}(0,t)|^2$$

for almost every $t \in (t_k, t_{k+1})$, which proves the desired estimate. □

4.6. Uniform dwell-time

Theorem 1 (Uniform dwell-time and exclusion of Zeno behavior)**.** *Assume that Assumptions 1–3 hold and that the dynamic event-triggering mechanism is given by* (4.15)–(4.16)*. Let $\rho_1', \alpha_1', \alpha_2', \alpha_3'$ be the constants in Lemma 7. Suppose that*

$$c_i > \frac{\alpha_i'}{\kappa}, \qquad i = 1, 2, 3. \tag{4.21}$$

Define

$$\theta_* := \max_{1\le i\le 3} \frac{\alpha_i'}{\kappa c_i}. \tag{4.22}$$

Then, $\theta_* < 1$. For any fixed $\theta \in (\theta_*, 1)$, there exists a constant $\tau_\theta > 0$ independent of the event index k and the initial condition such that every finite interevent interval satisfies

$$t_{k+1} - t_k \ge \tau_\theta. \tag{4.23}$$

Consequently, Zeno behavior is excluded.

Proof. Fix an interevent interval $[t_k, t_{k+1})$. If $t_{k+1} = \infty$, there is nothing to prove. Hence, suppose that $t_{k+1} < \infty$.
On the interevent interval, define

$$s_k(t) := \frac{e_U^2(t)}{-\kappa\zeta(t)}, \qquad t \in [t_k, t_{k+1}). \tag{4.24}$$

By Lemma 6, $\zeta(t) < 0$; hence, the denominator in (4.24) is strictly positive. Moreover,

$$s_k(t_k) = 0, \qquad 0 \le s_k(t) < 1, \quad t \in [t_k, t_{k+1}).$$

Using the pre-update value at the triggering instant, we extend s_k continuously to t_{k+1} by setting

$$s_k(t_{k+1}) = \frac{e_U^2(t_{k+1}^-)}{-\kappa\zeta(t_{k+1})} = 1.$$

For almost every $t \in (t_k, t_{k+1})$, differentiating (4.24) yields

$$\dot{s}_k(t) = \frac{1}{-\kappa\zeta(t)}\frac{d}{dt}(e_U^2(t)) + \frac{e_U^2(t)}{\kappa\zeta^2(t)}\dot{\zeta}(t).$$

Using Lemma 7,

$$\frac{d}{dt}(e_U^2(t)) \le \rho_1' e_U^2(t) + \sum_{i=1}^{3} \alpha_i' Z_i(t),$$

where

$$Z_1(t) := \|\hat{z}_x[t]\|^2, \qquad Z_2(t) := |\hat{z}(1,t)|^2, \qquad Z_3(t) := |\tilde{z}(0,t)|^2$$

together with

$$\dot{\zeta}(t) = -a_\zeta\zeta(t) + b_\zeta e_U^2(t) - \sum_{i=1}^{3} c_i Z_i(t)$$

and the identity

$$e_U^2(t) = -\kappa\zeta(t)s_k(t),$$

we obtain

$$\dot{s}_k(t) \le \kappa b_\zeta s_k^2(t) + (a_\zeta + \rho_1')s_k(t) + \sum_{i=1}^{3}\left(\frac{\alpha_i'}{\kappa} - c_i s_k(t)\right)\frac{Z_i(t)}{-\zeta(t)}. \tag{4.25}$$

Because $\theta_* < \theta < 1$, one has

$$\frac{\alpha_i'}{\kappa} - c_i\theta < 0, \qquad i = 1, 2, 3.$$

Because $s_k(t_k) = 0$, $s_k(t_{k+1}) = 1$, and s_k is continuous on $[t_k, t_{k+1}]$, the level θ is attained at least once. Define the last crossing time by

$$t_{k,\theta} := \max\{t \in [t_k, t_{k+1}] : s_k(t) = \theta\}. \tag{4.26}$$

By continuity and the definition of $t_{k,\theta}$, one has

$$s_k(t) \ge \theta, \qquad t \in [t_{k,\theta}, t_{k+1}].$$

Consequently,

$$\frac{\alpha_i'}{\kappa} - c_i s_k(t) \le \frac{\alpha_i'}{\kappa} - c_i\theta < 0, \qquad i = 1, 2, 3.$$

Because $Z_i(t) \geq 0$ and $-\zeta(t) > 0$, the state-dependent terms in (4.25) are nonpositive on $[t_{k,\theta}, t_{k+1}]$. Therefore, for almost every $t \in (t_{k,\theta}, t_{k+1})$,

$$\dot{s}_k(t) \leq \kappa b_\zeta s_k^2(t) + (a_\zeta + \rho_1')s_k(t). \tag{4.27}$$

Let

$$A := \kappa b_\zeta, \qquad B := a_\zeta + \rho_1'$$

so that $A > 0$, and $B > 0$. Define

$$F(r) := \int_\theta^r \frac{d\xi}{A\xi^2 + B\xi}, \qquad r \in [\theta, 1].$$

Because $s_k(t) \geq \theta > 0$ on $[t_{k,\theta}, t_{k+1}]$, the denominator is strictly positive. For almost every $t \in (t_{k,\theta}, t_{k+1})$, (4.27) gives

$$\frac{d}{dt}F(s_k(t)) = \frac{\dot{s}_k(t)}{As_k^2(t) + Bs_k(t)} \leq 1.$$

Integrating over $[t_{k,\theta}, t_{k+1}]$ yields

$$\int_\theta^1 \frac{ds}{As^2 + Bs} \leq t_{k+1} - t_{k,\theta} \leq t_{k+1} - t_k.$$

Therefore,

$$t_{k+1} - t_k \geq \tau_\theta,$$

where

$$\tau_\theta := \int_\theta^1 \frac{ds}{\kappa b_\zeta s^2 + (a_\zeta + \rho_1')s}. \tag{4.28}$$

Evaluating the integral gives

$$\tau_\theta = \frac{1}{a_\zeta + \rho_1'} \ln\left(\frac{a_\zeta + \rho_1' + \kappa b_\zeta \theta}{\theta\left(a_\zeta + \rho_1' + \kappa b_\zeta\right)}\right). \tag{4.29}$$

Because $0 < \theta < 1$,

$$a_\zeta + \rho_1' + \kappa b_\zeta \theta - \theta\left(a_\zeta + \rho_1' + \kappa b_\zeta\right) = (a_\zeta + \rho_1')(1 - \theta) > 0.$$

Hence, $\tau_\theta > 0$. The constant τ_θ depends only on the fixed design parameters and the constants in Lemma 7 but not on the event index k or the initial condition. Therefore, no infinite sequence of triggering instants can accumulate in finite time, and Zeno behavior is excluded. □

5. Mean-square exponential stability analysis

5.1. Lyapunov functional

Recall that the notation $\|f[t]\|$ has been defined in (4.16) as

$$\|f[t]\|^2 := \|f(\cdot, t)\|^2_{L^2(0,1)} = \int_0^1 f^2(x, t)\, dx.$$

Consider the Lyapunov functional

$$V(t) = \frac{A}{2}\|\tilde{z}[t]\|^2 + \frac{B}{2}\|\hat{z}[t]\|^2 - \gamma\zeta(t), \qquad A, B, \gamma > 0, \tag{5.1}$$

where $\gamma > 0$ is an additional weighting parameter used to balance the contribution of the internal triggering variable in the subsequent stability analysis. By Lemma 6, $\zeta(t) < 0$ for all $t \geq 0$, and hence, $-\gamma\zeta(t) > 0$. Therefore,

$$V(t) \geq \frac{A}{2}\|\tilde{z}[t]\|^2 + \frac{B}{2}\|\hat{z}[t]\|^2 \geq \frac{C_0}{2}\left(\|\tilde{z}[t]\|^2 + \|\hat{z}[t]\|^2\right), \qquad C_0 := \min\{A, B\}. \tag{5.2}$$

For later use, we record the boundary gradient estimates employed in the Lyapunov analysis. For every $z(\cdot, t) \in H^1(0, 1)$, the fundamental theorem of calculus gives

$$z(0, t) = z(1, t) - \int_0^1 z_x(x, t)\, dx.$$

Hence, by the Cauchy–Schwarz inequality,

$$|z(0, t)|^2 \leq 2\|z_x[t]\|^2 + 2|z(1, t)|^2. \tag{5.3}$$

Similarly, using $z(x, t) = z(1, t) - \int_x^1 z_x(\xi, t)\, d\xi$ and integrating over $x \in (0, 1)$ yields

$$\|z[t]\|^2 \leq 2\|z_x[t]\|^2 + 2|z(1, t)|^2. \tag{5.4}$$

Consequently, for every $a > 0$,

$$\|z_x[t]\|^2 + a|z(1, t)|^2 \geq \frac{1}{2}\min\{1, a\}\|z[t]\|^2. \tag{5.5}$$

In particular, define

$$D_{\tilde{z}}(t) := \|\tilde{z}_x[t]\|^2 + q|\tilde{z}(1, t)|^2, \qquad D_{\hat{z}}(t) := \|\hat{z}_x[t]\|^2 + r|\hat{z}(1, t)|^2. \tag{5.6}$$

By Assumption 1 together with the standing conditions $\varepsilon > 0$ and $\lambda > 0$, one has $q > 1/2$ and $r > 1/2$. Hence, define

$$M_q := \max\left\{1, \frac{1}{q}\right\}, \qquad M_r := \max\left\{1, \frac{1}{r}\right\}. \tag{5.7}$$

Then, (5.3)–(5.4) imply

$$|\tilde{z}(0, t)|^2 \leq 2M_q D_{\tilde{z}}(t), \qquad \|\tilde{z}[t]\|^2 \leq 2M_q D_{\tilde{z}}(t), \tag{5.8}$$

and

$$|\hat{z}(0, t)|^2 \leq 2M_r D_{\hat{z}}(t), \qquad \|\hat{z}[t]\|^2 \leq 2M_r D_{\hat{z}}(t). \tag{5.9}$$

These estimates retain the spatial gradient and right-boundary dissipation explicitly and will be used below to estimate boundary traces without bounding them by the L^2-state norm alone.

5.2. Mean-square stability criterion

Theorem 2 (Mean-square exponential stability)**.** *Assume that Assumptions 1–3 hold and that the dynamic event-triggering mechanism is given by* (4.15)–(4.16) *with* $\zeta_0 < 0$*. Suppose that there exist* $\delta_i > 0$*,* $i = 1, 2, 3$*, such that with the corresponding constants* α_i'*,* $i = 1, 2, 3$ *defined in Lemma 7,*

$$c_i > \frac{\alpha_i'}{\kappa}, \qquad i = 1, 2, 3. \tag{5.10}$$

Suppose further that there exist $A, B > 0$ *and* $\eta_j > 0$*,* $j = 1, \dots, 5$*. For brevity, define*

$$C_\Delta := \frac{A^2\|b\|^2_{L^2(0,1)}M_q}{2\eta_1} + \frac{A^2\varepsilon^2 b_0^2 M_q}{2\eta_2}, \qquad C_w := \frac{B^2\lambda^2 M_r}{8\eta_4} + \frac{B^2\|g\|^2_{L^2(0,1)}M_r}{2\eta_5}, \qquad C_e := \frac{B^2\varepsilon^2}{4\eta_3 r}.$$

Set

$$\nu_{\tilde{z}} := A\varepsilon - \eta_1 - \eta_2 - 4(1-P_g)^2(L_\varphi+1)^2 M_q C_\Delta, \qquad \nu_{\hat{z}} := B\varepsilon - \eta_3 - \eta_4 - \eta_5 - 8(1-P_g)^2(L_\varphi+1)^2 M_r C_w,$$

$$C_{\tilde{z}\hat{z}} := 4(1-P_g)^2(L_\varphi+1)^2 M_r C_\Delta, \qquad C_{\hat{z}\tilde{z}} := 4(1+2(1-P_g)^2(L_\varphi+1)^2) M_q C_w,$$

and

$$d_{\tilde{z}} := \nu_{\tilde{z}} - C_{\hat{z}\tilde{z}}, \qquad d_{\hat{z}} := \nu_{\hat{z}} - C_{\tilde{z}\hat{z}}, \qquad m_c := \max\left\{c_1, \frac{c_2}{r}\right\}.$$

Assume that the following joint feasibility condition holds:

$$\frac{C_e}{b_\zeta} < \min\left\{\frac{d_{\tilde{z}}}{2c_3M_q}, \frac{d_{\hat{z}}}{m_c}\right\}. \tag{5.11}$$

For any γ *satisfying*

$$\frac{C_e}{b_\zeta} < \gamma < \min\left\{\frac{d_{\tilde{z}}}{2c_3M_q}, \frac{d_{\hat{z}}}{m_c}\right\}, \tag{5.12}$$

define

$$\eta_{\tilde{z}} := d_{\tilde{z}} - 2\gamma c_3 M_q, \qquad \eta_{\hat{z}} := d_{\hat{z}} - \gamma m_c, \qquad \eta_e := \gamma b_\zeta - C_e.$$

Then, $\eta_{\tilde{z}} > 0$*,* $\eta_{\hat{z}} > 0$*, and* $\eta_e > 0$*. Let*

$$\rho := \min\left\{\frac{\eta_{\tilde{z}}}{AM_q}, \frac{\eta_{\hat{z}}}{BM_r}, a_\zeta\right\} > 0.$$

Then, the plant and observer states satisfy a global mean-square exponential estimate with respect to the augmented initial energy. More precisely, there exists a constant $C > 0$ *independent of the initial data such that for every admissible deterministic initial condition,*

$$\mathbb{E}\left\{\|v[t]\|^2 + \|\hat{v}[t]\|^2\right\} \le Ce^{-\rho t}\left(\|v_0\|^2 + \|\hat{v}_0\|^2 + (-\zeta_0)\right), \qquad t \ge 0. \tag{5.13}$$

Moreover, there exists a constant $C_\zeta > 0$ *independent of the initial data such that*

$$\mathbb{E}\{-\zeta(t)\} \le C_\zeta e^{-\rho t}\left(\|v_0\|^2 + \|\hat{v}_0\|^2 + (-\zeta_0)\right), \qquad t \ge 0.$$

Proof. For convenience, write the Lyapunov functional defined in (5.1) as

$$V(t) = V_1(t) + V_2(t) + V_3(t),$$

where

$$V_1(t) = \frac{A}{2}\|\tilde{z}[t]\|^2, \qquad V_2(t) = \frac{B}{2}\|\hat{z}[t]\|^2, \qquad V_3(t) = -\gamma\zeta(t).$$

Hence,

$$\dot{V}(t) = \dot{V}_1(t) + \dot{V}_2(t) - \gamma\dot{\zeta}(t).$$

Estimate of $\dot{V}_1(t)$. Using (3.11)–(3.13) together with (3.14), one has

$$\dot{V}_1(t) = A\int_0^1 \tilde{z}(x,t)\tilde{z}_t(x,t)\,dx = A\varepsilon\int_0^1 \tilde{z}(x,t)\tilde{z}_{xx}(x,t)\,dx + A\Delta_y(t)\int_0^1 b(x)\tilde{z}(x,t)\,dx.$$

Integrating by parts and using (3.12)–(3.13) yield:

$$\dot{V}_1(t) = -A\varepsilon\|\tilde{z}_x[t]\|^2 - A\varepsilon q|\tilde{z}(1,t)|^2 - A\varepsilon b_0\Delta_y(t)\tilde{z}(0,t) + A\Delta_y(t)\int_0^1 b(x)\tilde{z}(x,t)\,dx.$$

By the definition of $D_{\tilde{z}}(t)$ in (5.6), this becomes

$$\dot{V}_1(t) = -A\varepsilon D_{\tilde{z}}(t) - A\varepsilon b_0\Delta_y(t)\tilde{z}(0,t) + A\Delta_y(t)\int_0^1 b(x)\tilde{z}(x,t)\,dx.$$

We next estimate the attack-induced measurement deviation. By (3.10), Assumption 3, one has

$$|\Delta_y(t)| \le (1-P_g)(L_\varphi+1)|v(0,t)|.$$

Because the Volterra transformations reduce to the identity at $x = 0$,

$$\tilde{v}(0,t) = \tilde{z}(0,t), \qquad \hat{v}(0,t) = \hat{z}(0,t),$$

and hence,

$$v(0,t) = \tilde{z}(0,t) + \hat{z}(0,t).$$

It follows that

$$\Delta_y^2(t) \le 2(1-P_g)^2(L_\varphi+1)^2\left(|\tilde{z}(0,t)|^2 + |\hat{z}(0,t)|^2\right) \le 4(1-P_g)^2(L_\varphi+1)^2\left[M_q D_{\tilde{z}}(t) + M_r D_{\hat{z}}(t)\right]. \quad (5.14)$$

For any $\eta_1 > 0$, by the Cauchy–Schwarz and Young inequalities,

$$\begin{aligned}\left|A\Delta_y(t)\int_0^1 b(x)\tilde{z}(x,t)\,dx\right| &\le A\|b\|_{L^2(0,1)}|\Delta_y(t)|\,\|\tilde{z}[t]\| \\ &\le A\|b\|_{L^2(0,1)}\sqrt{2M_q}\,|\Delta_y(t)|\sqrt{D_{\tilde{z}}(t)} \\ &\le \eta_1 D_{\tilde{z}}(t) + \frac{A^2\|b\|^2_{L^2(0,1)}M_q}{2\eta_1}\Delta_y^2(t).\end{aligned}$$

Similarly, for any $\eta_2 > 0$,

$$\left|A\varepsilon b_0 \Delta_y(t)\tilde{z}(0,t)\right| \le A\varepsilon|b_0| \sqrt{2M_q}\, |\Delta_y(t)| \sqrt{D_{\tilde{z}}(t)} \le \eta_2 D_{\tilde{z}}(t) + \frac{A^2\varepsilon^2 b_0^2 M_q}{2\eta_2}\Delta_y^2(t).$$

Define

$$C_\Delta := \frac{A^2\|b\|^2_{L^2(0,1)} M_q}{2\eta_1} + \frac{A^2\varepsilon^2 b_0^2 M_q}{2\eta_2}.$$

Combining the above estimates gives

$$\dot{V}_1(t) \le -\left(A\varepsilon - \eta_1 - \eta_2\right) D_{\tilde{z}}(t) + C_\Delta \Delta_y^2(t).$$

Using (5.14), we finally obtain

$$\dot{V}_1(t) \le -\nu_{\tilde{z}} D_{\tilde{z}}(t) + C_{\tilde{z}\hat{z}} D_{\hat{z}}(t), \tag{5.15}$$

where

$$\nu_{\tilde{z}} = A\varepsilon - \eta_1 - \eta_2 - 4(1-P_g)^2(L_\varphi+1)^2 M_q C_\Delta, \qquad C_{\tilde{z}\hat{z}} = 4(1-P_g)^2(L_\varphi+1)^2 M_r C_\Delta.$$

We now give the estimate of $\dot{V}_2(t)$. Define

$$w(t) := \tilde{z}(0,t) + \Delta_y(t).$$

For almost every $t \in (t_k, t_{k+1})$, using (4.7), (4.8), and (4.14), one has

$$\dot{V}_2(t) = B\int_0^1 \hat{z}(x,t)\hat{z}_t(x,t)\,dx = B\varepsilon\int_0^1 \hat{z}(x,t)\hat{z}_{xx}(x,t)\,dx + Bw(t)\int_0^1 g(x)\hat{z}(x,t)\,dx.$$

Integrating by parts gives

$$\dot{V}_2(t) = B\varepsilon\left[\hat{z}(x,t)\hat{z}_x(x,t)\right]_0^1 - B\varepsilon\|\hat{z}_x[t]\|^2 + Bw(t)\int_0^1 g(x)\hat{z}(x,t)\,dx.$$

Using $\hat{z}_x(0,t) = -\lambda/(2\varepsilon)w(t)$, and $\hat{z}_x(1,t) = -r\hat{z}(1,t) - e_U(t)$, we obtain

$$\dot{V}_2(t) = -B\varepsilon\|\hat{z}_x[t]\|^2 - B\varepsilon r|\hat{z}(1,t)|^2 - B\varepsilon e_U(t)\hat{z}(1,t) + \frac{B\lambda}{2}\hat{z}(0,t)w(t) + Bw(t)\int_0^1 g(x)\hat{z}(x,t)\,dx.$$

By the definition of $D_{\hat{z}}(t)$ in (5.6), this becomes

$$\dot{V}_2(t) = -B\varepsilon D_{\hat{z}}(t) - B\varepsilon e_U(t)\hat{z}(1,t) + \frac{B\lambda}{2}\hat{z}(0,t)w(t) + Bw(t)\int_0^1 g(x)\hat{z}(x,t)\,dx.$$

We first estimate $w(t)$. By its definition,

$$w^2(t) \le 2|\tilde{z}(0,t)|^2 + 2\Delta_y^2(t).$$

Using (5.8) and (5.14), it follows that

$$w^2(t) \le 4M_q D_{\tilde{z}}(t) + 8(1-P_g)^2(L_\varphi+1)^2\left[M_q D_{\tilde{z}}(t) + M_r D_{\hat{z}}(t)\right]$$

$$= 4(1 + 2(1 - P_g)^2(L_\varphi + 1)^2)M_q D_{\tilde{z}}(t) + 8(1 - P_g)^2(L_\varphi + 1)^2 M_r D_{\hat{z}}(t).$$

For any $\eta_3 > 0$, because $r|\hat{z}(1,t)|^2 \leq D_{\hat{z}}(t)$, Young's inequality yields

$$B\varepsilon|e_U(t)|\,|\hat{z}(1,t)| \leq \frac{B\varepsilon}{\sqrt{r}}|e_U(t)|\sqrt{D_{\hat{z}}(t)} \leq \eta_3 D_{\hat{z}}(t) + \frac{B^2\varepsilon^2}{4\eta_3 r}e_U^2(t).$$

Similarly, for any $\eta_4 > 0$, using (5.9), one obtains

$$\frac{B|\lambda|}{2}|\hat{z}(0,t)|\,|w(t)| \leq \frac{B|\lambda|}{2}\sqrt{2M_r}\,|w(t)|\sqrt{D_{\hat{z}}(t)} \leq \eta_4 D_{\hat{z}}(t) + \frac{B^2\lambda^2 M_r}{8\eta_4}w^2(t).$$

Moreover, because $g \in L^\infty(0,1) \subset L^2(0,1)$, for any $\eta_5 > 0$, the Cauchy–Schwarz and Young inequalities give

$$\begin{aligned}\left|Bw(t)\int_0^1 g(x)\hat{z}(x,t)\,dx\right| &\leq B\|g\|_{L^2(0,1)}|w(t)|\,\|\hat{z}[t]\| \\ &\leq B\|g\|_{L^2(0,1)}\sqrt{2M_r}\,|w(t)|\sqrt{D_{\hat{z}}(t)} \\ &\leq \eta_5 D_{\hat{z}}(t) + \frac{B^2\|g\|^2_{L^2(0,1)}M_r}{2\eta_5}w^2(t).\end{aligned}$$

Define

$$C_w := \frac{B^2\lambda^2 M_r}{8\eta_4} + \frac{B^2\|g\|^2_{L^2(0,1)}M_r}{2\eta_5}, \qquad C_e := \frac{B^2\varepsilon^2}{4\eta_3 r}.$$

Combining the above estimates gives

$$\dot{V}_2(t) \leq -\left(B\varepsilon - \eta_3 - \eta_4 - \eta_5\right) D_{\hat{z}}(t) + C_e e_U^2(t) + C_w w^2(t).$$

Substituting the preceding estimate of $w^2(t)$ yields

$$\dot{V}_2(t) \leq -\Big(B\varepsilon-\eta_3-\eta_4-\eta_5-8(1-P_g)^2(L_\varphi+1)^2 M_r C_w\Big)D_{\hat{z}}(t)+4(1+2(1-P_g)^2(L_\varphi+1)^2)M_q C_w D_{\tilde{z}}(t)+C_e e_U^2(t).$$

Define

$$\nu_{\hat{z}} := B\varepsilon - \eta_3 - \eta_4 - \eta_5 - 8(1 - P_g)^2(L_\varphi + 1)^2 M_r C_w$$

and

$$C_{\hat{z}\tilde{z}} := 4(1 + 2(1 - P_g)^2(L_\varphi + 1)^2)M_q C_w.$$

Therefore, for almost every $t \in (t_k, t_{k+1})$,

$$\dot{V}_2(t) \leq -\nu_{\hat{z}} D_{\hat{z}}(t) + C_{\hat{z}\tilde{z}} D_{\tilde{z}}(t) + C_e e_U^2(t). \tag{5.16}$$

The coefficients in (5.16) will be combined with those in (5.15) in the subsequent coupled stability estimate.

Combining (5.15) and (5.16), for almost every $t \in (t_k, t_{k+1})$, we obtain

$$\dot{V}_1(t) + \dot{V}_2(t) \leq -\nu_{\tilde{z}} D_{\tilde{z}}(t) + C_{\tilde{z}\hat{z}} D_{\hat{z}}(t) - \nu_{\hat{z}} D_{\hat{z}}(t) + C_{\hat{z}\tilde{z}} D_{\tilde{z}}(t) + C_e e_U^2(t).$$

Define

$$d_{\tilde{z}} := \nu_{\tilde{z}} - C_{\hat{z}\tilde{z}}, \qquad d_{\hat{z}} := \nu_{\hat{z}} - C_{\tilde{z}\hat{z}}.$$

Then,

$$\dot{V}_1(t) + \dot{V}_2(t) \le -d_{\tilde{z}} D_{\tilde{z}}(t) - d_{\hat{z}} D_{\hat{z}}(t) + C_e e_U^2(t). \tag{5.17}$$

The above estimate will next be combined with the contribution of $V_3(t) = -\gamma\zeta(t)$ to obtain the final dissipation inequality.
We now give the estimate of $\dot{V}_3(t)$. Because $V_3(t) = -\gamma\zeta(t)$, using (4.16) gives

$$\dot{V}_3(t) = \gamma a_\zeta \zeta(t) - \gamma b_\zeta e_U^2(t) + \gamma c_1 \|\hat{z}_x[t]\|^2 + \gamma c_2 |\hat{z}(1,t)|^2 + \gamma c_3 |\tilde{z}(0,t)|^2.$$

Because $\zeta(t) < 0$ by Lemma 6, one has $-\zeta(t) > 0$, and hence,

$$\dot{V}_3(t) = -\gamma a_\zeta(-\zeta(t)) - \gamma b_\zeta e_U^2(t) + \gamma c_1 \|\hat{z}_x[t]\|^2 + \gamma c_2 |\hat{z}(1,t)|^2 + \gamma c_3 |\tilde{z}(0,t)|^2.$$

To combine these terms with (5.17), define

$$m_c := \max\left\{c_1, \frac{c_2}{r}\right\}.$$

Then, by the definition of $D_{\hat{z}}(t)$,

$$c_1 \|\hat{z}_x[t]\|^2 + c_2 |\hat{z}(1,t)|^2 \le m_c D_{\hat{z}}(t).$$

Moreover, from (5.8),

$$c_3 |\tilde{z}(0,t)|^2 \le 2 c_3 M_q D_{\tilde{z}}(t).$$

Combining the above estimates with (5.17) for almost every $t \in (t_k, t_{k+1})$ yields

$$\dot{V}(t) \le -\left(d_{\tilde{z}} - 2\gamma c_3 M_q\right) D_{\tilde{z}}(t) - \left(d_{\hat{z}} - \gamma m_c\right) D_{\hat{z}}(t) - \left(\gamma b_\zeta - C_e\right) e_U^2(t) - \gamma a_\zeta(-\zeta(t)).$$

Define

$$\eta_{\tilde{z}} := d_{\tilde{z}} - 2\gamma c_3 M_q, \qquad \eta_{\hat{z}} := d_{\hat{z}} - \gamma m_c, \qquad \eta_e := \gamma b_\zeta - C_e.$$

Hence,

$$\dot{V}(t) \le -\eta_{\tilde{z}} D_{\tilde{z}}(t) - \eta_{\hat{z}} D_{\hat{z}}(t) - \eta_e e_U^2(t) - \gamma a_\zeta(-\zeta(t)). \tag{5.18}$$

For the subsequent stability estimate, we require

$$\eta_{\tilde{z}} > 0, \qquad \eta_{\hat{z}} > 0, \qquad \eta_e > 0.$$

These requirements will be incorporated into the joint feasibility conditions of the stability criterion.
We now derive the exponential decay estimate. From (5.8) and (5.9), one has

$$D_{\tilde{z}}(t) \ge \frac{1}{2M_q} \|\tilde{z}[t]\|^2, \qquad D_{\hat{z}}(t) \ge \frac{1}{2M_r} \|\hat{z}[t]\|^2.$$

Therefore, by (5.18) and $\eta_e > 0$,

$$\dot{V}(t) \le -\frac{\eta_{\tilde{z}}}{2M_q} \|\tilde{z}[t]\|^2 - \frac{\eta_{\hat{z}}}{2M_r} \|\hat{z}[t]\|^2 - \gamma a_\zeta(-\zeta(t)).$$

Define
$$\rho := \min\left\{\frac{\eta_{\tilde{z}}}{AM_q}, \frac{\eta_{\hat{z}}}{BM_r}, a_\zeta\right\} > 0.$$
Then,
$$\frac{\eta_{\tilde{z}}}{2M_q} \geq \frac{\rho A}{2}, \qquad \frac{\eta_{\hat{z}}}{2M_r} \geq \frac{\rho B}{2}, \qquad \gamma a_\zeta \geq \rho\gamma.$$
Recalling that
$$V(t) = \frac{A}{2}\|\tilde{z}[t]\|^2 + \frac{B}{2}\|\hat{z}[t]\|^2 + \gamma(-\zeta(t)),$$
we consequently obtain, for almost every $t \in (t_k, t_{k+1})$,
$$\dot{V}(t) \leq -\rho V(t). \tag{5.19}$$
Under the standing regularity assumptions, the transformed PDE states have the time regularity required for the above energy estimates, whereas $\zeta(t)$ is absolutely continuous on each interevent interval. Consequently, $V(t)$ is absolutely continuous on each interevent interval. Moreover, the PDE states remain continuous at the triggering instants, and $\zeta(t)$ is not reset; hence, $V(t)$ is continuous at every t_k. By Theorem 1, Zeno behavior is excluded, so the triggering instants do not accumulate in finite time. Because (5.19) holds for almost every $t \in (t_k, t_{k+1})$, it follows that
$$\frac{d}{dt}\left(e^{\rho t}V(t)\right) = e^{\rho t}\left(\dot{V}(t) + \rho V(t)\right) \leq 0$$
for almost every $t \in (t_k, t_{k+1})$. Integrating over each interevent interval and using the continuity of $V(t)$ at the triggering instants yields
$$V(t) \leq e^{-\rho t}V(0), \qquad t \geq 0. \tag{5.20}$$
Taking expectations on both sides gives
$$\mathbb{E}\{V(t)\} \leq e^{-\rho t}\mathbb{E}\{V(0)\}.$$
Furthermore, from (5.2),
$$\|\tilde{z}[t]\|^2 + \|\hat{z}[t]\|^2 \leq \frac{2}{C_0}V(t), \qquad C_0 = \min\{A, B\}.$$
Therefore,
$$\mathbb{E}\left\{\|\tilde{z}[t]\|^2 + \|\hat{z}[t]\|^2\right\} \leq \frac{2}{C_0}e^{-\rho t}\mathbb{E}\{V(0)\}.$$
Finally, because the Volterra transformations (3.1)–(3.2) and (4.1) are boundedly invertible in $L^2(0,1)$, there exist constants $M_{\tilde{v}} > 0$ and $M_{\hat{v}} > 0$ such that
$$\|\tilde{v}[t]\| \leq M_{\tilde{v}}\|\tilde{z}[t]\|, \qquad \|\hat{v}[t]\| \leq M_{\hat{v}}\|\hat{z}[t]\|.$$
Because $v[t] = \tilde{v}[t] + \hat{v}[t]$, there exists a constant $M_V > 0$ such that
$$\|v[t]\|^2 + \|\hat{v}[t]\|^2 \leq M_V\left(\|\tilde{z}[t]\|^2 + \|\hat{z}[t]\|^2\right).$$

Consequently,

$$\mathbb{E}\left\{\|v[t]\|^2 + \|\hat{v}[t]\|^2\right\} \le \frac{2M_V}{C_0} e^{-\rho t}\mathbb{E}\{V(0)\}.$$

At the initial time,

$$V(0) = \frac{A}{2}\|\tilde{z}[0]\|^2 + \frac{B}{2}\|\hat{z}[0]\|^2 + \gamma(-\zeta_0).$$

Because the Volterra transformations are bounded in $L^2(0,1)$, and $\tilde{v}[0] = v_0 - \hat{v}_0$, there exists a constant $M_0 > 0$ independent of the initial data such that

$$\|\tilde{z}[0]\|^2 + \|\hat{z}[0]\|^2 \le M_0\left(\|v_0\|^2 + \|\hat{v}_0\|^2\right).$$

Hence, there exists a constant $C_V > 0$ independent of the initial data such that

$$V(0) \le C_V\left(\|v_0\|^2 + \|\hat{v}_0\|^2 + (-\zeta_0)\right).$$

For the deterministic initial data considered here, $\mathbb{E}\{V(0)\} = V(0)$. Therefore, for some constant $C > 0$ independent of the initial data,

$$\mathbb{E}\left\{\|v[t]\|^2 + \|\hat{v}[t]\|^2\right\} \le Ce^{-\rho t}\left(\|v_0\|^2 + \|\hat{v}_0\|^2 + (-\zeta_0)\right), \qquad t \ge 0. \tag{5.21}$$

Moreover, because $\gamma(-\zeta(t)) \le V(t)$, it follows from (5.20) that

$$\mathbb{E}\{-\zeta(t)\} \le \frac{C_V}{\gamma} e^{-\rho t}\left(\|v_0\|^2 + \|\hat{v}_0\|^2 + (-\zeta_0)\right), \qquad t \ge 0.$$

□

Remark 7. *The sufficient conditions in Theorem 2 require the dissipative contributions associated with the transformed estimation error and observer dynamics to dominate the coupling terms induced by measurement deception and event-triggered implementation. In particular, the joint feasibility condition* (5.11) *guarantees the existence of a weighting parameter* γ *such that* $\eta_{\tilde{z}} > 0$, $\eta_{\hat{z}} > 0$, *and* $\eta_e > 0$. *Thus, the admissible deception level and the triggering parameters must be selected jointly with the backstepping and Lyapunov parameters.*

6. Simulation results

We simulate the one-dimensional reaction–diffusion system (2.1)–(2.4), where the boundary measurement is taken at $x = 0$, and the control input is applied at $x = 1$. We choose $\varepsilon = 1.80$, $\lambda = 1.7292$, and $q = 1.45$. These values satisfy Assumption 1, and consequently, $r = q - \lambda/(2\varepsilon) = 0.9697$. The initial conditions are $v(x,0) = 2\sin(\pi x)$ and $\hat{v}(x,0) \equiv 0$ for $x \in [0,1]$. The spatial domain is uniformly discretized using $N_x = 51$ grid points, the time step is $\Delta t = 10^{-4}$ s, and the simulation horizon is $T = 12$ s. For the dynamic event-triggering mechanism, we select $\zeta_0 = -0.05$, $\kappa = 1.0$, $a_\zeta = 0.02$, $b_\zeta = 7.0$, and $c_1 = c_2 = 0.005$, $c_3 = 0.0005$. The genuine measurement probability is set to $P_g = 0.875$. The deception map is chosen as $\varphi(z) = 0.05\sin(z)$ with $L_\varphi = 0.05$, which satisfies Assumption 3. At each control update instant, a new Bernoulli mode is sampled according to P_g, and this mode is held constant over the corresponding interevent interval, consistent with the attack model introduced in Section 2. The event-triggered control input is updated only when the prescribed triggering condition is met and is held constant between consecutive triggering instants. For the Lyapunov function in Theorem 2, the weighting parameters are selected as $A = 10.4041$ and $B = 1$. Substitution of these parameters into the feasibility conditions of Theorem 2 gives the admissible range $4.7822 < \gamma < 6.6359$. Hence, $\gamma = 5.7090$ is selected, and all assumptions and feasibility conditions required by Theorem 2 are satisfied for the selected parameters.

Figure 1 compares the open-loop and closed-loop responses. As shown in Figure 1(a)–(b), the uncontrolled plant with $U(t) \equiv 0$ exhibits unstable behavior, with the state magnitude and the corresponding $L^2(0, 1)$ norm increasing rapidly with time. In contrast, Figure 1(c)–(d) shows that the proposed observer-based, event-triggered boundary control suppresses the unstable dynamics after the initial transient, and $\|v(\cdot, t)\|_{L^2(0,1)}$ decreases toward zero. This comparison illustrates the stabilizing effect of the proposed closed-loop scheme.

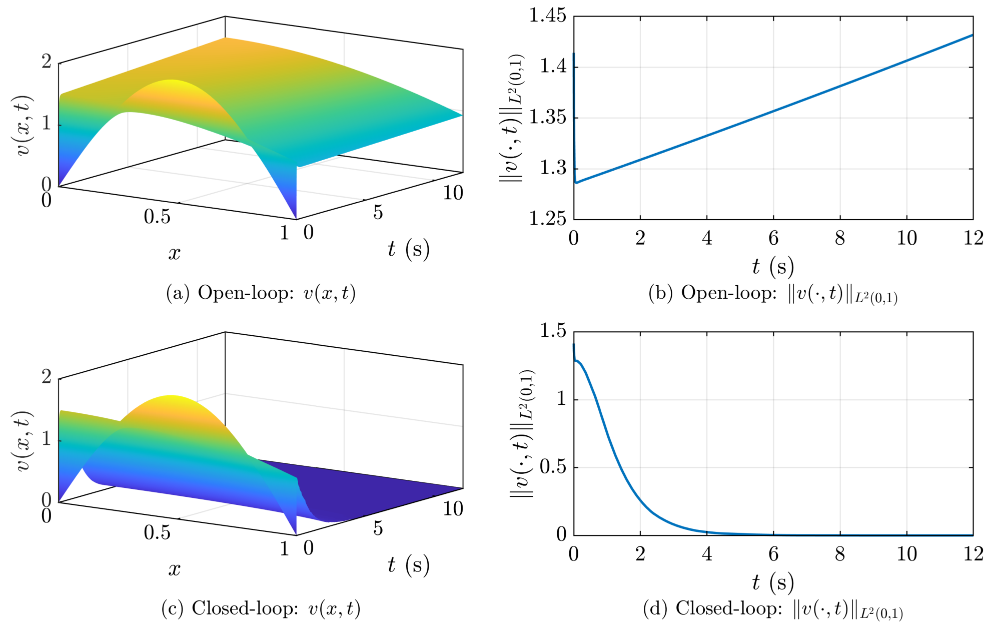

(a) Open-loop: $v(x,t)$ (b) Open-loop: $\|v(\cdot,t)\|_{L^2(0,1)}$

(c) Closed-loop: $v(x,t)$ (d) Closed-loop: $\|v(\cdot,t)\|_{L^2(0,1)}$

Figure 1. Open-loop versus event-triggered closed-loop responses.

Figure 2 illustrates the observer performance under random deceptive measurements by comparing the plant state $v(x, t)$ and the observer state $\hat{v}(x, t)$ at two representative spatial locations, $x = 0.24$ and $x = 0.74$. The shaded regions indicate intervals in which $\beta(t) = 0$, corresponding to deceptive measurements. Although the measurement channel is intermittently corrupted, the observer trajectories approach the corresponding plant-state trajectories after the initial transient, and both the plant and observer states decay toward zero. The numerical results therefore illustrate effective state reconstruction of the proposed boundary observer in the presence of random deceptive measurements.

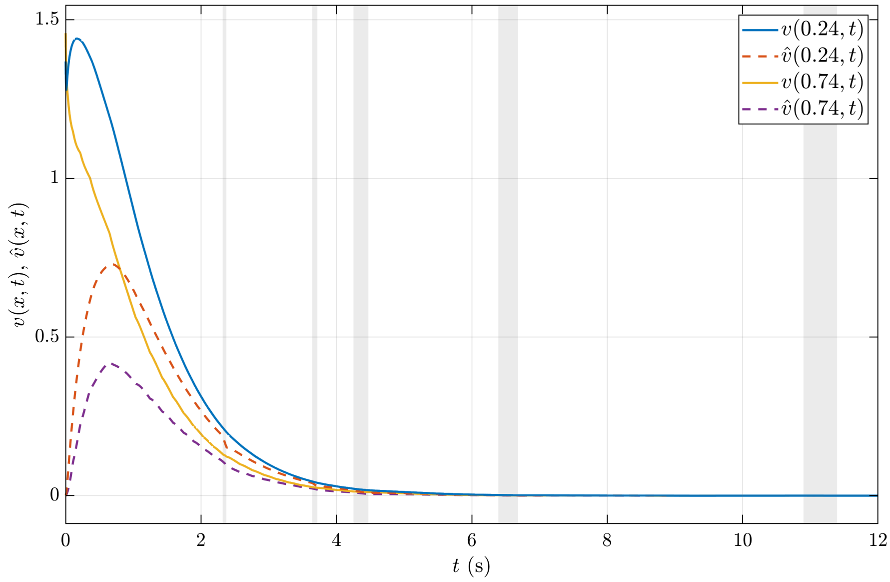

Figure 2. Observer performance under random deceptive measurements.

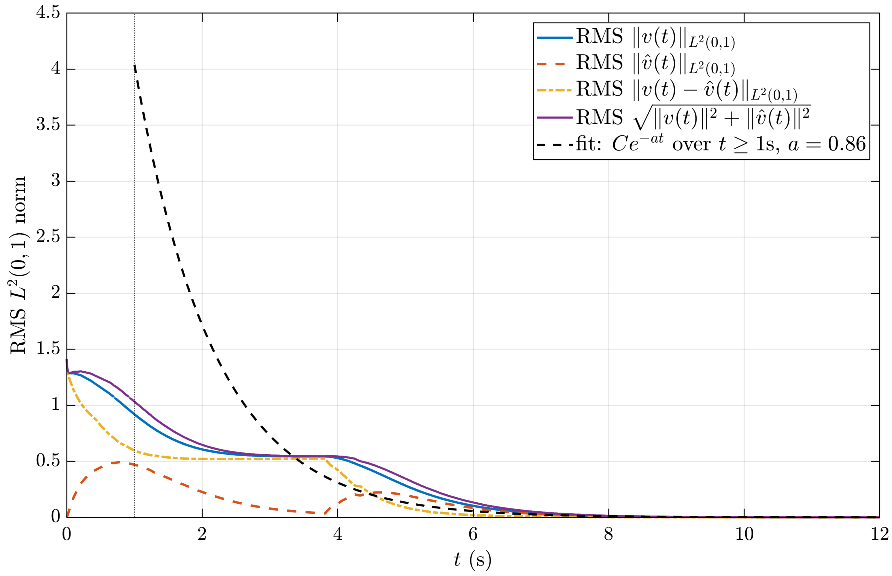

Figure 3. Monte Carlo RMS convergence under random deceptive measurements.

To further illustrate the closed-loop behavior under random deceptive measurements, we perform a Monte Carlo study using 30 independent attack realizations. For each realization, the same system, controller, and event-triggering parameters are used. Figure 3 reports the ensemble root mean square (RMS) trajectories of $\|v(t)\|_{L^2(0,1)}$, $\|\hat{v}(t)\|_{L^2(0,1)}$, and $\|v(t) - \hat{v}(t)\|_{L^2(0,1)}$ together with the combined RMS state measure $\sqrt{\mathbb{E}\left\{\|v(t)\|^2_{L^2(0,1)} + \|\hat{v}(t)\|^2_{L^2(0,1)}\right\}}$. The RMS quantities exhibit an overall decreasing trend after the initial transient and approach small values as time evolves. For reference, an exponential curve of the form Ce^{-at} is fitted to the combined RMS state measure over $t \geq 1$ s and is included in the figure. These Monte Carlo results provide numerical evidence of the convergence behavior of the proposed closed-loop scheme under random deceptive measurements.

We next examine the interevent times generated by the dynamic event-triggering mechanism. For the selected parameters, the numerical constants associated with Theorem 2 are $\rho_1' = 15972.9$ and $\alpha_1' = \alpha_2' = 0.0025$, $\alpha_3' = 0.00025$. Hence, $c_i > \alpha_i'/\kappa$, $i = 1, 2, 3$, is satisfied. In particular, $\theta_* = 0.5$. Choosing $\theta = 0.75 \in (\theta_*, 1)$ gives the analytical dwell-time lower bound $\tau_\theta = 1.8 \times 10^{-5}$ s.

Figure 4 shows the interevent times $\Delta_k = t_{k+1} - t_k$ together with this analytical lower bound. Over the simulated trajectory, the minimum and maximum observed interevent times are $\min_k \Delta_k = 0.0541$ s, $\max_k \Delta_k = 2.5245$ s, respectively. These numerical results are consistent with the positive dwell-time estimate established in Theorem 1 and illustrate the absence of arbitrarily fast triggering in the simulation.

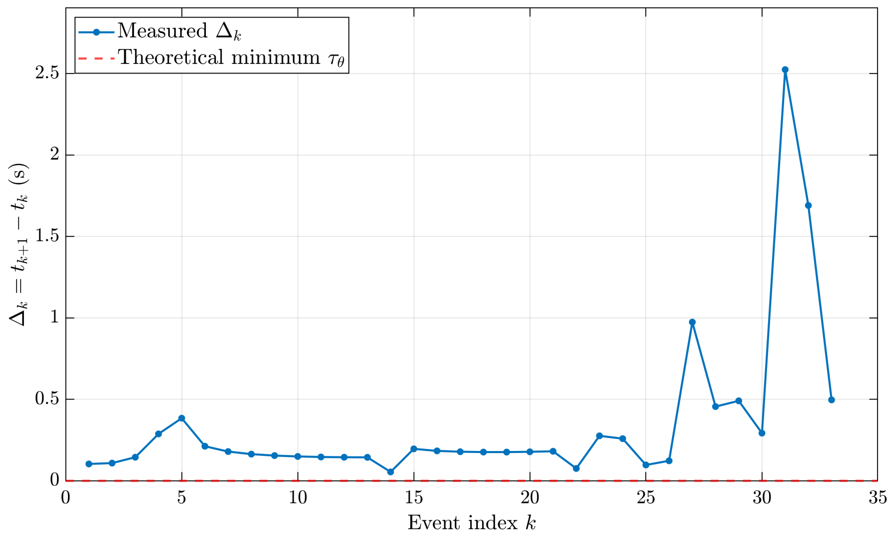

Figure 4. Interevent times and the analytical dwell-time lower bound.

Figure 5 further illustrates the interaction between random deceptive measurements and the dynamic event-triggering mechanism. Figure 5(a) shows the Bernoulli mode $\beta(t)$, where the shaded regions correspond to deceptive-measurement intervals $\beta(t) = 0$. Figure 5(b) provides a compressed view of the triggering quantities by plotting $(e_U^2(t)/\kappa)^{0.2}$ and $(-\zeta(t))^{0.2}$ together with the triggering instants. The trigger markers are determined using the pre-update value of the input-holding error, consistent with the event condition $e_U^2(t^-) \geq -\kappa\zeta(t)$. Figure 5(c) compares the estimation error norm $\|v(t) - \hat{v}(t)\|_{L^2(0,1)}$ for the case with random deceptive measurements using $P_g = 0.875$ and the attack-free case $\beta(t) \equiv 1$. The deceptive-measurement case exhibits larger transient estimation errors over some attack intervals, whereas the attack-free trajectory is generally smoother. Nevertheless, both estimation error trajectories remain bounded and decrease with time. This comparison illustrates the closed-loop tolerance to intermittent measurement deception under the considered simulation setting.

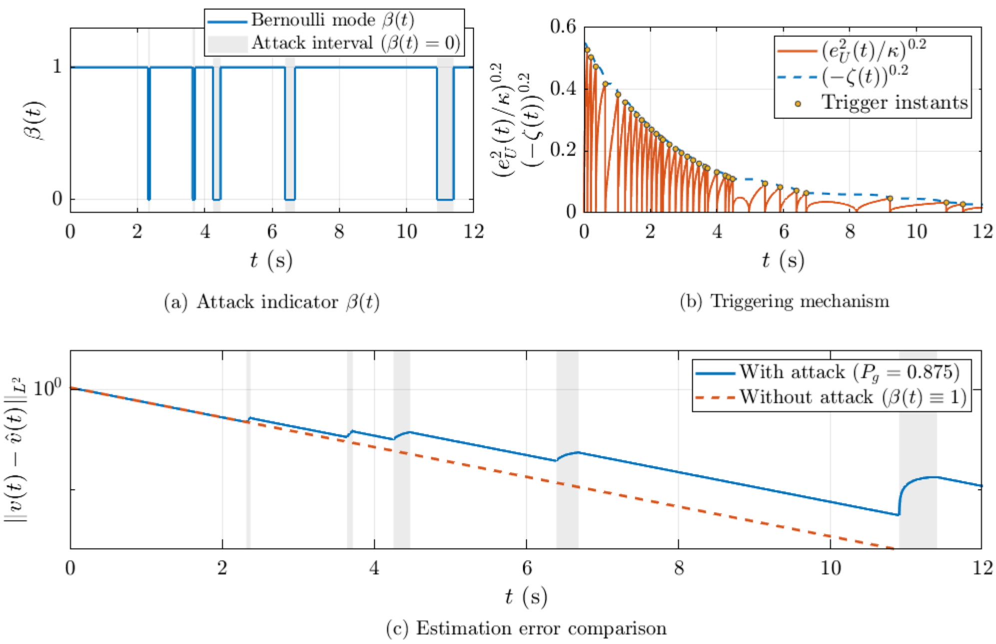

Figure 5. Attack robustness and triggering behavior.

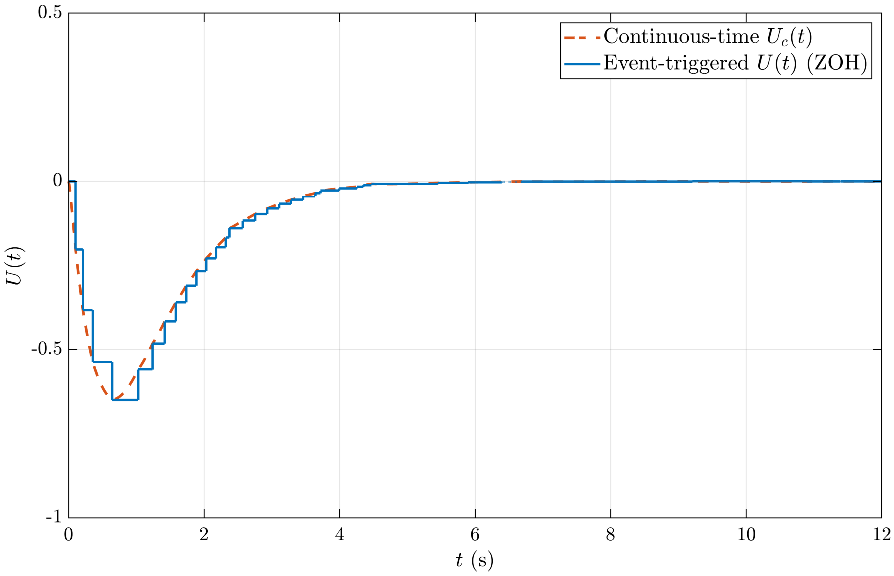

Figure 6. Boundary control input comparison.

Finally, Figure 6 compares the ideal continuous-time boundary feedback signal $U_c(t)$ with its event-triggered sample-and-hold implementation $U(t)$. The implemented input $U(t)$ is piecewise constant and is updated only at the triggering instants, whereas $U_c(t)$ evolves continuously. The two signals remain close over the simulation horizon, particularly after the initial transient. As the closed-loop state approaches the equilibrium, both signals approach zero, and the control updates become increasingly sparse. This behavior illustrates that the proposed event-triggered implementation can track the ideal continuous-time boundary feedback while avoiding continuous control updates.

7. Conclusions

We have investigated boundary output feedback stabilization for a one-dimensional reaction–diffusion system under random deceptive measurement attacks. The attacked boundary measurement has been modeled by a Bernoulli switching process together with a Lipschitz deception map, which captures intermittent falsification while retaining analytical tractability. A unified backstepping-based framework has been developed to simultaneously address boundary output feedback stabilization, sampled data or event-triggered actuation, and stochastic deception on the sensing channel. Specifically, a boundary observer together with its associated output feedback control law was derived, and a fully dynamic triggering strategy regulated by an auxiliary internal variable has been introduced to adapt the triggering threshold online. Key properties have been rigorously established, including the forward invariance of $\zeta(t) < 0$ and Zeno exclusion via a positive lower bound on the spacing between successive events, together with verifiable conditions yielding a global mean-square exponential estimate for the plant and observer states with respect to the augmented initial energy through a coupled Lyapunov functional that integrates the plant state, observer error, and triggering dynamics. Numerical simulations have corroborated robust stabilization and accurate estimation under attacks while significantly reducing boundary input updates after transients.

Several directions for future work have been identified. The proposed methodology can be extended to more general parabolic PDEs and higher-dimensional domains, and richer network or attack effects (e.g., noise, delays or quantization, and Markovian or mixed attack models) can be incorporated. In addition, adaptive tuning of triggering parameters and implementation-oriented validation have been considered as promising steps toward improving the control update–performance tradeoff and supporting practical deployment.

Author contributions

Lianglin Xiong: Funding acquisition, Supervision, Writing–review & editing; Xueqing Chen: Conceptualization, Methodology, Formal analysis, Investigation, Writing–original draft; Haiyang Zhang: Validation; Tao Wu: Methodology, Visualization. All authors reviewed and approved the final version of the manuscript.

Use of Generative-AI tools declaration

The author declares that the use of AI tools, specifically ChatGPT, was limited to language editing and checking the logical consistency of certain mathematical arguments. All scientific content, proofs, results, and conclusions were developed and independently verified by the author, who takes full responsibility for the work.

Acknowledgments

This research was supported by the National Natural Science Foundation of China under grants 12061088 and 12426611, the Yunnan Provincial Basic Research Program under grants 202401AT070969 and 202201AU070046, and the Open Foundation of Yunnan Key Laboratory of Intelligent Control and Application under grant 2025ICA04.

Conflict of interest

All authors declare no conflicts of interest in this paper.

References

1. A. Smyshlyaev, M. Krstic, Backstepping observers for a class of parabolic PDEs, *Syst. Control Lett.*, **54** (2005), 613–625. http://doi.org/10.1016/j.sysconle.2004.11.001
2. G. A. de Andrade, R. Vazquez, D. J. Pagano, Backstepping-based estimation of thermoacoustic oscillations in a Rijke tube with experimental validation, *IEEE Trans. Automat. Contr.*, **65** (2020), 5336–5343. http://doi.org/10.1109/TAC.2020.2970152
3. H. Anfinsen, O. M. Aamo, Stabilization of a linear hyperbolic PDE with actuator and sensor dynamics, *Automatica*, **95** (2018), 104–111. http://doi.org/10.1016/j.automatica.2018.05.019
4. M. Krstic, A. Smyshlyaev, *Boundary control of PDEs: a course on backstepping designs*, Philadelphia, PA: Society for Industrial and Applied Mathematics, 2008. http://doi.org/10.1137/1.9780898718607
5. G. Weiss, Admissibility of unbounded control operators, *SIAM J. Control Optim.*, **27** (1989), 527–545. http://doi.org/10.1137/0327028
6. H. Lhachemi, C. Prieur, Finite-dimensional observer-based boundary stabilization of reaction-diffusion equations with either a Dirichlet or Neumann boundary measurement, *Automatica*, **135** (2022), 109955. http://doi.org/10.1016/j.automatica.2021.109955
7. J. Li, Y. Ding, New mechanism for spatial heterogeneity pattern revealed by nonlocal competition and host-taxis in a 2D pine wilt disease model, *J. Math. Biol.*, **92** (2026), 19. http://doi.org/10.1007/s00285-025-02336-4
8. Y. Ding, P. Yu, Equivalence of MTS and CMR methods on the normal form of Turing-Hopf bifurcation in delayed reaction–diffusion equations, *Chaos Soliton. Fract.*, **202** (2026), 117485. http://doi.org/10.1016/j.chaos.2025.117485
9. R. Vazquez, M. Krstic, Explicit boundary control of reaction-diffusion PDEs on arbitrary-dimensional balls, In: *2015 European control conference (ECC)*, Linz, Austria, 2015, 879–884. http://doi.org/10.1109/ECC.2015.7330653
10. T. Hashimoto, M. Krstic, Stabilization of reaction diffusion equations with state delay using boundary control input, *IEEE Trans. Automat. Contr.*, **61** (2016), 4041–4047. http://doi.org/10.1109/TAC.2016.2539001
11. C. Peng, F. Li, A survey on recent advances in event-triggered communication and control, *Inform. Sciences*, **457–458** (2018), 113–125. http://doi.org/10.1016/j.ins.2018.04.055

12. X.-M. Zhang, Q.-L. Han, B.-L. Zhang, An overview and deep investigation on sampled-data-based event-triggered control and filtering for networked systems, *IEEE Trans. Ind. Inform.*, **13** (2017), 4–16. http://doi.org/10.1109/TII.2016.2607150
13. I. Karafyllis, M. Krstic, Sampled-data boundary feedback control of 1-D parabolic PDEs, *Automatica*, **87** (2018), 226–237. http://doi.org/10.1016/j.automatica.2017.10.006
14. P. Tabuada, Event-triggered real-time scheduling of stabilizing control tasks, *IEEE Trans. Automat. Contr.*, **52** (2007), 1680–1685. http://doi.org/10.1109/TAC.2007.904277
15. W. P. M. H. Heemels, M. C. F. Donkers, A. R. Teel, Periodic event-triggered control for linear systems, *IEEE Trans. Automat. Contr.*, **58** (2013), 847–861. http://doi.org/10.1109/TAC.2012.2220443
16. A. Girard, Dynamic triggering mechanisms for event-triggered control, *IEEE Trans. Automat. Contr.*, **60** (2015), 1992–1997. http://doi.org/10.1109/TAC.2014.2366855
17. M. Abdelrahim, R. Postoyan, J. Daafouz, D. Nešić, Robust event-triggered output feedback controllers for nonlinear systems, *Automatica*, **75** (2017), 96–108. http://doi.org/10.1016/j.automatica.2016.09.044
18. N. Espitia, A. Girard, N. Marchand, C. Prieur, Event-based control of linear hyperbolic systems of conservation laws, *Automatica*, **70** (2016), 275–287. http://doi.org/10.1016/j.automatica.2016.04.009
19. A. Selivanov, E. Fridman, Distributed event-triggered control of diffusion semilinear PDEs, *Automatica*, **68** (2016), 344–351. http://doi.org/10.1016/j.automatica.2016.02.006
20. M. Wakaiki, H. Sano, Event-triggered control of infinite-dimensional systems, *SIAM J. Control Optim.*, **58** (2020), 605–635. http://doi.org/10.1137/18M1179717
21. B. Rathnayake, M. Diagne, Global exponential stability of event-triggered control of a parabolic PDE with switching dynamic triggering designs, *IMA J. Math. Control Inform.*, **42** (2025), dnaf042. http://doi.org/10.1093/imamci/dnaf042
22. D. Ding, Q.-L. Han, Y. Xiang, X. Ge, X.-M. Zhang, A survey on security control and attack detection for industrial cyber-physical systems, *Neurocomputing*, **275** (2018), 1674–1683. http://doi.org/10.1016/j.neucom.2017.10.009
23. A. Teixeira, I. Shames, H. Sandberg, K. H. Johansson, A secure control framework for resource-limited adversaries, *Automatica*, **51** (2015), 135–148. http://doi.org/10.1016/j.automatica.2014.10.067
24. S.-R. Jia, W.-J. Lin, Adaptive event-triggered reachable set control for Markov jump cyber-physical systems with time-varying delays, *AIMS Math.*, **9** (2024), 25127–25144. http://doi.org/10.3934/math.20241225
25. D. Zhao, Z. Wang, G. Wei, Q.-L. Han, A dynamic event-triggered approach to observer-based PID security control subject to deception attacks, *Automatica*, **120** (2020), 109128. http://doi.org/10.1016/j.automatica.2020.109128
26. Y. Deng, Z. Meng, H. Lu, Adaptive event-triggered state estimation for complex networks with nonlinearities against hybrid attacks, *AIMS Math.*, **7** (2022), 2858–2877. http://doi.org/10.3934/math.2022158

27. H. Fawzi, P. Tabuada, S. Diggavi, Secure estimation and control for cyber-physical systems under adversarial attacks, *IEEE Trans. Automat. Contr.*, **59** (2014), 1454–1467. http://doi.org/10.1109/TAC.2014.2303233
28. N. Shukla, N. Keerthana, R. Sakthivel, V. T. Elayabharath, J. Dabas, Observer-reliant event-triggered security control design for stochastic third-order PDE systems with multiple attacks, *Eur. J. Control*, **82** (2025), 101186. http://doi.org/10.1016/j.ejcon.2025.101186
29. B. Rathnayake, M. Diagne, N. Espitia, I. Karafyllis, Observer-based event-triggered boundary control of a class of reaction-diffusion PDEs, *IEEE Trans. Automat. Contr.*, **67** (2022), 2905–2917. http://doi.org/10.1109/TAC.2021.3094648
30. F. Koudohode, N. Espitia, M. Krstic, Event-triggered boundary control of an unstable reaction diffusion PDE with input delay, *Syst. Control Lett.*, **186** (2024), 105775. http://doi.org/10.1016/j.sysconle.2024.105775
31. H. Yuan, J. Wang, J. Zeng, W. Lan, Output-feedback event-triggered boundary control of reaction-diffusion PDEs with delayed actuator, *Automatica*, **176** (2025), 112266. http://doi.org/10.1016/j.automatica.2025.112266
32. N. Espitia, J. Auriol, Event-triggered gain scheduling of 2×2 linear hyperbolic PDEs with time and space varying coupling coefficients, *Automatica*, **179** (2025), 112455. http://doi.org/10.1016/j.automatica.2025.112455
33. Y. Xiao, X. Xu, B. Luo, C. Yang, W. Gui, Adaptive event-triggered tracking control for strict-feedback nonlinear ODE cascaded $n+1$ coupled hyperbolic PDE systems, *ISA Trans.*, **164** (2025), 24–33. http://doi.org/10.1016/j.isatra.2025.05.019
34. Z. Chen, J. Tan, Y. He, Z. Cao, Decentralized observer-based event-triggered control for an interconnected fractional-order system with stochastic cyber-attacks, *AIMS Math.*, **9** (2024), 1861–1876. http://doi.org/10.3934/math.2024091
35. S. Touhami, A. Chaira, D. F. M. Torres, Harmonic and trace inequalities in Lipschitz domains, In: *Frontiers in functional equations and analytic inequalities*, Cham: Springer, 2019, 599–611. http://doi.org/10.1007/978-3-030-28950-8_30
36. J. M. Steele, *The Cauchy-Schwarz master class: an introduction to the Art of mathematical inequalities*, Cambridge: Cambridge University Press, 2004.
37. E. D. Sontag, Y. Wang, New characterizations of input-to-state stability, *IEEE Trans. Automat. Contr.*, **41** (1996), 1283–1294. http://doi.org/10.1109/9.536498
38. I. Karafyllis, M. Krstic, *Input-to-state stability for PDEs*, Cham: Springer, 2019. http://doi.org/10.1007/978-3-319-91011-6
39. V. V. Kravchenko, *Direct and inverse Sturm-Liouville problems: a method of solution*, Cham: Birkhäuser, 2020. http://doi.org/10.1007/978-3-030-47849-0